urban science

MDPI

Article

Outdoor Thermal Comfort of Older People in Vulnerable Urban Areas in a Warming World: Evidence from Porto, Portugal

Md Imtiaz Ahmad [1,*], Rachita Klinmalee [1], Helena Corvacho [2,*], Franklin Gaspar [1], Paulo Conceição [1], Sara Cruz [1], Luísa Batista [1], Cecília Rocha [1], Fernando Alves [1], Anabela Salgueiro Narciso Ribeiro [1], Rui Jorge Garcia Ramos [3], Gisela Lameira [3], Ana Martins [3], Ana S. Fernandes [3], Joel Bruno da Silva [4], Teodora Figueiredo [4], Luís Midão [4], Leovaldo Alcântara [4], Inês Mimoso [4] and Elísio Costa [4]

[1] CITTA—Research Centre for Territory, Transport and Environment, Faculty of Engineering, University of Porto, 4200-465 Porto, Portugal; rachitaklin@gmail.com (R.K.); up202204098@edu.fe.up.pt (F.G.); psc@fe.up.pt (P.C.); scruz@fe.up.pt (S.C.); lbatista@fe.up.pt (L.B.); carocha@fe.up.pt (C.R.); alves@fe.up.pt (F.A.); anabela@dec.uc.pt (A.S.N.R.)

[2] CONSTRUCT—Institute of R&D in Structures and Construction, Faculty of Engineering, University of Porto, 4200-465 Porto, Portugal

[3] CENP—Nuno Portas Centre for Studies, Faculty of Architecture, University of Porto, 4150-564 Porto, Portugal; rramos@arq.up.pt (R.J.G.R.); glameira@arq.up.pt (G.L.); amartins@arq.up.pt (A.M.); alfernandes@arq.up.pt (A.S.F.)

[4] RISE—Health, Competence Center for Active and Healthy Ageing, Faculty of Pharmacy, University of Porto, 4050-313 Porto, Portugal; jbruno@ff.up.pt (J.B.d.S.); tgfigueiredo@ff.up.pt (T.F.); lmidao@ff.up.pt (L.M.); lsalcantara@ff.up.pt (L.A.); ifmimoso@ff.up.pt (I.M.)

* Correspondence: up202202072@edu.fe.up.pt (M.I.A.); corvacho@fe.up.pt (H.C.)

Abstract

Amid growing concerns over global warming, ensuring the outdoor thermal comfort (OTC) of public urban spaces is crucial for creating liveable and resilient cities. This study focused on the intensification of the urban heat island (UHI) effect and the heat stress experienced by the vulnerable older population. Evidence was found through the case study in a highly vulnerable area of Porto, with a high ageing ratio. The primary aim was to assess the influence of design-based adaptation strategies on OTC using ENVI-met, with a specific focus on older adults. Thermal stress was evaluated using the Physiological Equivalent Temperature (PET) index. The analysis confirms that older adults consistently experience higher PET values (+2–5 °C) and larger areas of thermal discomfort than active-age adults. Simulations reveal that the effectiveness of adaptation measures depends on the characteristics of the urban space but enhanced green infrastructure achieves the most significant heat mitigation results. Artificial shading only provides localized thermal relief. Cool pavements contribute meaningfully by lowering surface heat storage and reducing longwave radiation. However, their impact on PET, beneficial or detrimental, depends significantly on the morphology of the outdoor space and the materials used. In the analysed street canyon, PET was higher in the central hours of the day for both age ranges, when the pavement material had a higher albedo. An effective heat mitigation needs a combination of vegetation-based strategies and climate-responsive materials to ensure comfortable and age-inclusive public spaces. This research presents an actionable methodological approach for evaluating and enhancing OTC, advocating the use of microclimate simulations in a carefully selected set of public spaces within an intervention urban area to define effective climate adaptation measures for each space.

Keywords: urban heat island; climate adaptation; thermal comfort; vulnerable older population; microclimate simulation

Check for updates

Academic Editor: Marialena Nikolopoulou

Received: 20 January 2026
Revised: 15 February 2026
Accepted: 7 March 2026
Published: 5 May 2026

1. Introduction

European urban areas have seen a significant population increase in recent years [1]. Currently, around 75% of the European population resides in urban areas, and this proportion is projected to rise to more than 80% in the coming decades [2]. In Portugal, the urban population accounts for approximately 68% of the total population and is expected to increase to around 80% by 2050. The global rise in urbanisation and the resulting densification of urban areas have significant impacts on the environment, human health, and overall well-being. The buildings and paved surfaces, combined with densely built-up infrastructure and a decline in vegetation and permeable public open spaces, contribute to the negative effects of human CO_2 emissions on climate change, which subsequently affects the population's daily lives [3].

The urban heat island (UHI) effect is recognised and extensively studied as one of the most significant phenomena amplified by climate change in recent decades [4,5]. UHI refers to the well-documented condition where urban areas exhibit significantly higher outdoor air temperatures (up to 12 K higher) than their surrounding rural or less urbanised regions [6,7]. This temperature disparity is primarily linked to specific features of urban environments, such as high building density, structure size and orientation, the layout of open spaces, and the widespread use of heat-retaining construction materials such as concrete and asphalt [8–10]. Moreover, other urban challenges, like air pollution and anthropogenic heat sources (such as industry, transportation), significantly enhance the thermal load within the urban canopy layer [11].

Thus, the collective impacts of rapid urban growth, urban features that intensify thermal stress, and the accelerating effects of climate change create significant challenges for urban environments, underscoring the urgent necessity to investigate resilience strategies to mitigate elevated urban temperatures [12]. Existing research in this field has predominantly focused on understanding the dynamics of UHI, diminished outdoor thermal comfort (OTC), and degraded air quality while also considering urban planning and design strategies aimed at addressing and alleviating these climatic challenges [13–15]. To create sustainable age-friendly urban environments, planners and designers must integrate both local and global climate considerations into their design processes, taking into account the long-term consequences of climate change in shaping resilient urban futures [16].

The concepts of exposure, vulnerability, and diverse perception have been much less explored in the literature of this research field. During periods of extreme heat, older people face higher vulnerability due to age-related physiological changes that reduce their thermoregulatory capacity, thereby increasing their susceptibility to heat-related illnesses. The prevalence of chronic health conditions, including cardiovascular, respiratory, and metabolic diseases, heightens this risk [17,18]. Moreover, inadequate housing, poor living conditions, and limited access to healthcare, often linked to low socioeconomic conditions, compound these vulnerabilities and amplify the adverse impacts of climate change. In this context, public spaces assume a vital role, not only as areas for recreation and social interaction but also as protective environments that help mitigate the harmful effects of heat exposure and promote the well-being of older urban residents.

The "Climate Adaptation for Older People Living in Vulnerable Urban Areas: Designing a Climate-Responsive and Community-Based Methodology (CAOP)" project (REF.PTDC/GES-URB/2038/2021), within which this paper was produced, tries to fill the identified research gap, aiming to address and mitigate some of the negative impacts of climate change, namely the ones related to high temperatures, on older adults living in vulnerable urban areas, by bringing together experts from different fields, such as civil engineering, architecture, urban planning, ethnographic studies, and health. Within this broader framework of the CAOP project, this paper presents part of the research carried

https://doi.org/10.3390/urbansci10050249

out, investigating microclimatic variations that affect OTC across three residential zones characterised by distinct urban morphologies in *São Roque da Lameira*, Porto, Portugal, a neighbourhood identified as particularly vulnerable to climate-related stressors in which lives a population that is also vulnerable (older adults and low income). Using ENVI-met V5.7.2 software, microclimatic simulations were conducted under summer conditions for each spatial configuration.

A substantial body of literature has demonstrated the effectiveness of Computational Fluid Dynamics (CFD) models in examining the influence of urban morphology on local microclimates across diverse climatic and spatial contexts. Among these, ENVI-met is one of the most widely utilised tools for simulating urban environments [19,20]. It integrates and accounts for spatial variations in four primary microclimate variables: air temperature, mean radiant temperature, relative humidity, and wind speed, which collectively shape thermal comfort. Significant existing research supports the conclusion that ENVI-met provides a comprehensive framework for investigating the relationship between urban design parameters, microclimatic conditions, and thermal comfort. OTC was evaluated using the Physiological Equivalent Temperature (PET) index, an essential indicator of human thermal perception, particularly relevant to older populations in urban contexts. The goal of the study was to assess the urban microclimate within the selected sites and test climate adaptation strategies to foster healthy, liveable, and age-friendly outdoor environments that enhance urban resilience to excessive heat.

Although the application of adaptation measures to elevated urban temperatures has been widely explored in previous studies, this research represents an original analysis conducted for the selected area within the city of Porto and focusing on older residents. This research aims to test possible strategies that can be implemented by planners, designers, and urban decision-makers to counter the UHI effects intensified by climate change, considering the vulnerability of the users and their various perceptions. By exposing the methodology used for a case study and showing the results for three sites with different morphology, orientation, used materials and existing vegetation, this study demonstrates the need for the careful selection of a set of public spaces within a future intervention area in order to test the real effectiveness of potential adaptation measures, through simulation, for each specific space.

2. Background and State-of-the-Art

2.1. Outdoor Thermal Comfort (OTC)

Both climatic variables and human factors influence thermal comfort in outdoor urban spaces [21]. The degree and nature of activities occurring in public open spaces are closely linked to how comfortable or uncomfortable individuals feel under existing weather conditions. There has been an increasing focus on understanding OTC, primarily driven by rapid urbanisation and development, as well as the growing impacts of climate change, including the intensification of the UHI effect. To evaluate thermal comfort in specific microclimatic conditions, researchers have developed a variety of thermal comfort indices. Some well-known indices include the Outdoor Standard Effective Temperature (OUT_SET) [22,23], the Physiologically Equivalent Temperature (PET) [24,25], and the Universal Thermal Climate Index (UTCI) [26,27]. Although originally developed for the indoor environment, the Predicted Mean Vote (PMV) [28] is also used. Among all the mentioned indices, PET has proven to be particularly valuable [29,30].

PET represents the air temperature in a typical indoor setting (free from wind or solar radiation) where a person's heat balance and physiological responses, including core and skin temperatures, match those experienced under complex outdoor climatic conditions [25]. One of PET's main advantages lies in its universal applicability. Because

https://doi.org/10.3390/urbansci10050249

it is based on human thermophysiology, PET provides a realistic reflection of thermal perception. Expressed in degrees Celsius, it is easy to interpret and compare with everyday temperature experiences. To assess human thermal comfort, in addition to the microclimatic conditions of a specific space, PET considers the user's biological gender, age, clothing, and activity. Furthermore, it remains objective and versatile, functioning effectively across both warm and cool climates [31].

Research by Matzarakis et al. [32] explored the use of PET in evaluating the thermal characteristics of urban microclimates, particularly in forested zones near urban cores. Their findings confirmed that PET is a reliable tool for the biometeorological evaluation of thermal environments across diverse climatic regions. Table 1 presents the PET-based thermal comfort classification for Western and Central Europe, along with the corresponding thermal sensations and physiological stress levels.

Table 1. PET Classification.

PET (°C)	Thermal Sensation	Physiological Stress Level
<4	Very cold	Extreme cold stress
4–8	Cold	Strong cold stress
8–13	Cool	Moderate cold stress
13–18	Slightly cool	Slight cold stress
18–23	Comfortable	No thermal stress
23–29	Slightly warm	Slight heat stress
29–35	Warm	Moderate heat stress
35–41	Hot	Strong heat stress
>41	Very hot	Extreme heat stress

2.2. Microclimate Variables

Air temperature (Ta) is widely recognised as the primary determinant of OTC. It exerts a direct and easily perceptible influence on human thermal perception and is often the most dominant parameter in comfort assessments [33–35].

Wind speed (Ws) has a complex influence on OTC. Wind facilitates convective cooling of the human body, thereby effectively mitigating the physiological heat load. Furthermore, it modulates the surrounding thermal conditions by cooling urban surfaces in contact with the outdoor environment [36]. Additionally, it can also enhance psychological comfort by fostering a perceived sense of freshness. Its impact depends on several factors, including the intensity, directionality, and fluctuations of the wind, as well as the individual's location, body posture, and metabolic rate (activity level).

Relative humidity (RH), in contrast, is typically considered the least influential environmental factor in determining OTC. Its primary effect is to condition evaporative heat loss and respiratory heat exchange. Nevertheless, high RH can significantly worsen discomfort in hot conditions [37] by suppressing the efficiency of sweat evaporation, making it more difficult for the body to regulate its temperature.

The mean radiant temperature (MRT) is a key parameter for evaluating human thermal exposure as it offers a vital summary of the radiation exchange between the human body and its surrounding built and natural environment [38–41]. Direct solar radiation can generate significant thermal discomfort during summer, while in winter, it may enhance comfort levels. Especially in summer, MRT is a primary factor driving spatial variation in human thermal comfort [42] and is an essential parameter in numerous thermal comfort indices that include radiative exposure. MRT encompasses all shortwave and longwave radiation fluxes, both direct and reflected, and depends on the temperature of the surrounding objects and surfaces that influence the human body's thermal experience. MRT is defined as the value of the uniform temperature of an imaginary enclosure in which the radiant heat exchange with the user is equal to the radiant heat exchange in the actual non-uniform environment.

2.3. Urban Morphology, Materials, and Greenery

Recent studies have examined how urban layout and UHI effects influence thermal comfort while also exploring appropriate mitigation strategies. The UHI effect demonstrates a significant correlation with both two-dimensional (2D) and three-dimensional (3D) urban morphological indicators. Although for different reasons, densely built areas with low sky view factor (SVF, percentage of sky that can be seen from a given location) and regions with a dispersed distribution of buildings with high SVF tend to mitigate UHI. In contrast, those with moderate SVF tend to aggravate it [43]. However, this cannot be taken as a universal rule. The closeness of buildings creates larger shaded areas but it also intensifies their mutual heat exchanges by radiation. These two effects coexist in a critical balance, depending on the outdoor space geometry and the materials used. A dispersed distribution of buildings has opposite effects, resulting in less shadow but reduced heat exchange between buildings. Thus, urban morphology optimization should focus on spatial specificity [43].

The physical properties of surface materials play a crucial role in shaping the UHI effect, as they govern how solar energy is absorbed, reflected, and emitted by outdoor surfaces. The solar reflectance or albedo of building envelopes and pavements is particularly important, influencing not only building energy performance during cooling periods [44,45] but also the microclimatic conditions within urban spaces. Surface materials significantly influence the local microclimate through their thermal properties. Most common paving materials exhibit low albedo (meaning they reflect only a small portion of incoming solar radiation) and tend to store heat effectively, while many building materials possess high emissivity. As a result, these surfaces act as primary heat sinks, absorbing substantial solar radiation during diurnal periods, which increases surface and air temperatures, and subsequently release stored heat at night, thereby contributing to elevated nocturnal temperatures.

Pavements comprise a large proportion of the urban fabric, significantly influencing the development of the UHI effect [46]. In Europe, urban pavements are predominantly made of concrete or asphalt, materials that reach high surface temperatures during summer. Reducing these temperatures can improve the thermal conditions in cities facing high urban heat stress. Potential interventions include the substitution of conventional pavements with materials exhibiting lower surface temperatures or by retrofitting existing pavements to enhance their reflective and thermal performance. Another effective strategy is shading paved areas, which reduces the absorption of solar radiation.

Cool pavements are designed to address these issues by incorporating high-albedo materials with elevated thermal emissivity (reflective pavements) or by using materials that promote evaporative cooling through water retention (water-retentive pavements) [44]. However, reflective pavements must be applied carefully, particularly in densely built environments. In such settings, reflected solar radiation may strike nearby façades, resulting in multiple reflections or the excessive heating of vertical surfaces, ultimately undermining pedestrian thermal comfort.

It is a well-known fact that permeable substrates, such as soil and grass, enhance urban thermal comfort more effectively than paved surfaces. In environments with higher vegetation density, both potential air temperatures and mean radiant temperatures are consistently lower. These green spaces serve as critical cooling agents in densely built areas, both by providing cooler surfaces and shading, as well as by air cooling via evapotranspiration. It is worth noting, however, that vegetation has a low albedo, but a portion of the absorbed solar radiation is used for photosynthesis.

The complex interaction between climatic factors and built environment features makes the assessment of OTC and of the effectiveness of some measures difficult to carry out without microclimate simulation.

2.4. Microclimate Simulation

Numerical models have become essential tools for analysing urban climates, supporting the work of engineers, designers, urban planners, and policymakers. Their importance lies in providing predictive insights for climate-responsive urban planning, allowing professionals to evaluate different urban layouts and climatic conditions [47], making it possible to compare various design alternatives and assess their environmental performance [48]. Additionally, they can simulate study areas under multiple meteorological scenarios, providing valuable information for developing planning strategies rooted in urban biometeorology.

A variety of computational tools have been established to model urban microclimates, such as Solweig, ENVI-met, RayMan, etc. [49]. Unlike weather station data, which provide limited spatial coverage, simulation models can generate detailed outputs for specific climatic parameters [48]. Prognostic CFD models enable comparisons of urban designs during the planning phase under various temporal and climatic conditions [50,51]. Microclimate models significantly enhance our ability to predict the detailed patterns of airflow, temperature, and other scalar fields, ranging from individual buildings to entire districts [52]. These models account for various factors, including radiation, evapotranspiration, sensible heat fluxes, and soil heat exchange. As a result, they are extremely valuable for assessing energy performance across urban areas [53].

Among these, prognostic models like ENVI-met, which are grounded in the physical principles of fluid dynamics and thermodynamics, stand out for their ability to conduct comparative analyses of different scenarios. Although these models rely on simplifications due to the complexity of urban microclimate processes, they provide reliable predictions for phenomena difficult to capture through direct observation. Numerous studies have demonstrated the usefulness of ENVI-met in urban assessments [19], including applications focused on cool materials and vegetation-based cooling strategies [54].

Existing academic literature has predominantly focused on examining urban microclimate and outdoor thermal sensations within single urban blocks or master plan developments in individual studies. However, there has been a notable absence of consideration for the diverse demographic groups and age ranges within the population, particularly older people, who are identified as the most vulnerable demographic subgroup. The proposed workflow offers a replicable methodology that can be used by both researchers and practitioners to assess urban microclimate conditions more effectively in their design and urban master planning.

3. Methodology

This study focused on adaptation strategies to be employed in urban public spaces across diverse residential settings. To assess (I) pedestrian comfort levels and (II) the performance of selected heat-stress mitigation techniques, this research conducted a literature review, collected field data, and performed software simulations of microclimate conditions (see Figure 1).

https://doi.org/10.3390/urbansci10050249

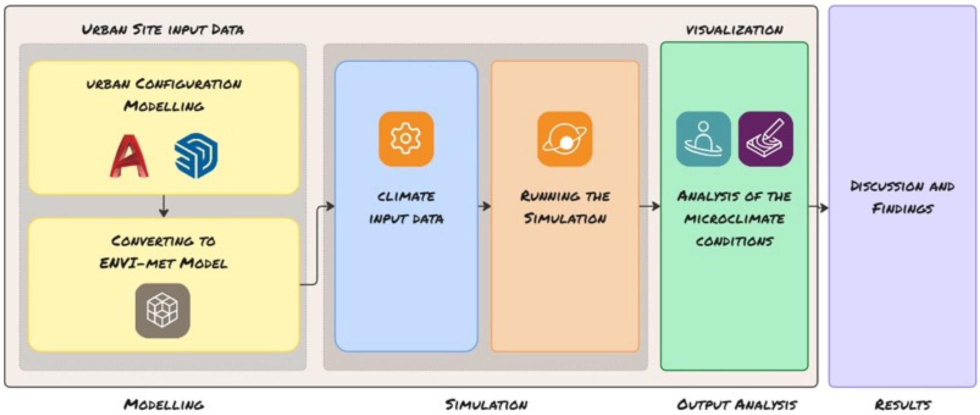

Figure 1. Stepwise graphical representation of the applied methodology.

To ensure a comprehensive analysis, the selection of three representative study zones was guided by a criteria-based approach to ensure morphological diversity. These criteria included:

1. A variation in residential typologies, ranging from single-family houses to multi-family buildings, with structures of various heights.
2. Presence of standardised urban voids within the residential fabric. Specifically, public open spaces between buildings and traditional urban canyons.
3. A variety of geographic orientations for both built structures and open spaces relative to the north to account for varying thermal exposure.

In this study, systematic field observations were conducted across three urban settings within the selected zones to identify and analyse physical morphology. This analysis incorporated several key aspects, including building form, construction materials, urban density, street orientation, and vegetation distribution. Based on these observations, three-dimensional models were created using the collected data. These models, built from urban morphological analysis, enable the visualisation of how buildings and outdoor features respond to external influences.

Each studied outdoor space was examined involving two distinct configurations: (1) the baseline scenario—original urban setting in its current state, and (2) an experimental scenario—a tested urban setting following modifications. These scenarios were compared to evaluate the effects of the transformations on the open space and their influence on the microclimate within each study site.

Although the simulations may not fully capture the intricate nature of real-world urban environments, they provide valuable comparative insights into microclimate parameters and their implications for urban design.

4. Case Study

4.1. Study Region and Case Study Area

This study investigated OTC in three selected zones of an urban area in Porto, Portugal. Porto is a coastal town in the northern region of Portugal and was home, in 2024, to approximately 253,000 residents [55]. Due to its geographical location, Porto experiences a temperate climate with Mediterranean characteristics (Köppen–Geiger classification, Csb), influenced by its proximity to the sea and the presence of mountainous elevations in the eastern interior. The climate is marked by dry, mild summers and cooler, rainy winters. However, extensive urbanisation, through changes in building form, density and height, as well as in ground cover and vegetation, significantly alters the local microclimatic conditions, leading to increased temperatures and modifications in wind direction and ventilation patterns. As with many cities worldwide, Porto is therefore facing growing

https://doi.org/10.3390/urbansci10050249

challenges related to climate change, reinforcing the need to account for the cumulative effects of urbanisation in urban design and climate adaptation strategies.

To identify urban areas susceptible to an intensified UHI effect, an examination of Porto's climate and urban scenario was conducted. The interpretation of thermal charts like the one in Figure 2 indicates the presence of a pronounced UHI effect in some areas of Porto [56]. The study area selected for this research is situated on the northeast side of the city (Figure 3), where high temperatures are typically reached in summer, making it an appropriate example for assessing heat-related vulnerabilities.

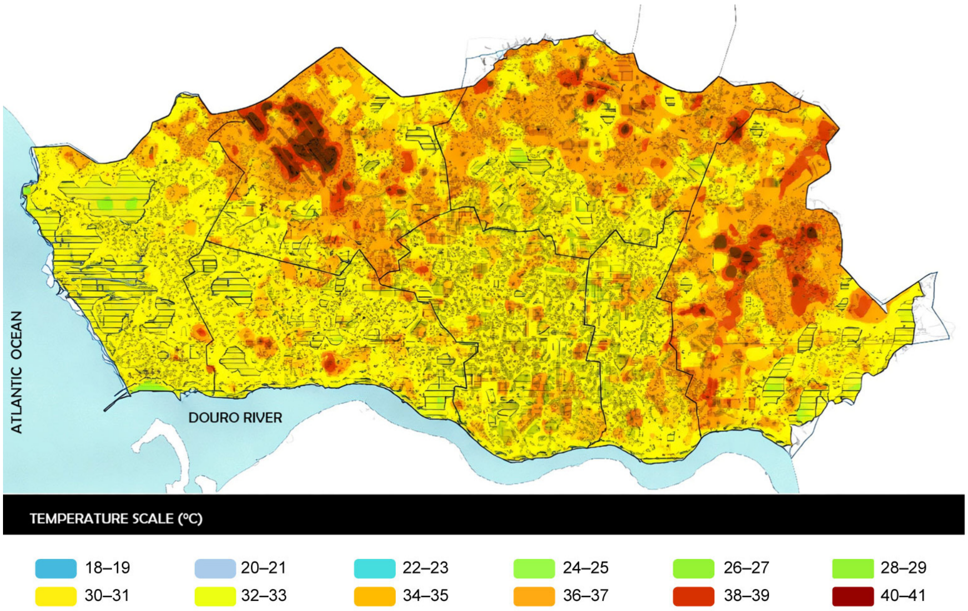

Figure 2. Example of a thermal chart of Porto on a day in August. Source: [56], reproduced and adapted with permission from Ana Monteiro, author of reference [56].

Figure 3. Location of the parish of *Campanhã*, the *ARU-Corujeira*, and the study area of *São Roque da Lameira* within the Municipality of Porto. Source: CAOP.

In alignment with the CAOP project's central focus on the ageing population, the case study selection was strategically focused on an area within Porto characterised by a significant concentration of older residents, specifically those aged 65 and over, who are around 31% of the entire population in the *São Roque da Lameira* area. The ageing ratio (number of people aged 65+ per 100 youngsters, 0–14 years old) in the Parish of *Campanhã*, where *São Roque da Lameira* area is located, was 231.7 in 2021 [57]. This selection was further refined by considering social vulnerability. This targeted approach ensures that the microclimate simulations directly address the environmental impacts pertinent to this ageing demographic.

The three selected zones to be assessed are situated in *São Roque da Lameira* area, in *Campanhã* parish, the easternmost parish of Porto. This area covers approximately 46 hectares and is part of a designated Urban Regeneration Area (*ARU*), specifically the *ARU of Corujeira*, which means that it is a priority for urban regeneration, as defined by the municipal council.

São Roque da Lameira faces socio-spatial vulnerabilities due to its physical and demographic structure, which is further aggravated by its peripheral placement within Porto. The area is geographically constrained by significant physical barriers, namely a major railway line and an extensive traffic road network, which contribute to its isolation and peripheral situation. The built environment includes a mix of public housing, precarious informal housing developments (‘*llhas*’), and derelict industrial spaces. The dense urban development, combined with the area’s topography (it is a valley) and the widespread use of industrial and road network materials, promotes substantial heat accumulation and prolonged heat retention. These factors, alongside high air pollution levels, heighten the area’s long-term climatic vulnerability.

The area also exhibits heterogeneous morphology, incorporating the historic, high-traffic corridor of *São Roque da Lameira* street (a mixed-use area with public transport and services) alongside primarily monofunctional residential neighbourhoods. These neighbourhoods feature a historic layout of single-family homes (*Grupo de Moradias Populares de São Roque da Lameira*, 1959/63) and multi-family buildings (*Bairro das Casas Económicas de Contumil*, 1942/48). These two types of buildings, with distinct characteristics—such as in form (geometry and volume) and construction (façade material)—were chosen to test a diversity of situations and present distinct responses to heat, as will be visible ahead in the simulation results. The prevalence of narrow streets and narrow sidewalks, coupled with old infrastructure and heavy traffic, significantly restricts mobility and walkability, posing notable challenges, particularly for the older population. This complex interplay of challenging physical conditions and high thermal risk makes *São Roque da Lameira* a priority area for study. In Figure 4, the zones chosen within the *São Roque da Lameira* area are identified.

The following is a breakdown of the micro-morphological characteristics of the different urban zones:

Urban zone of public space 1. This zone is characterised by a predominantly homogeneous urban configuration, consisting of multi-family social housing blocks. The buildings are typologically and morphologically consistent, structured as large urban complexes. A key feature is the presence of extensive open outdoor spaces, serving as community gathering areas and parking areas situated between the buildings.

Urban zone of public space 2. This zone presents a suburban residential fabric characterised by a mix of single-family houses. Its layout is distinguished by a curvilinear street pattern featuring multiple cul-de-sacs and looped streets. Central to this area is a vegetated space on the central island, a confluence of several streets.

Urban zone of public space 3. This zone follows a classic street canyon morphology along *São Roque da Lameira* street, functioning as a significant urban corridor. This zone is defined by a two-way, high-traffic street bordered by buildings of varying heights, predominantly comprising single-family homes. Additionally, there are unoccupied structures and buildings undergoing renovation.

The three selected zones represent the heterogeneous morphology of the *São Roque da Lameira* area and ensure the diversity of the studied sample.

Figure 4. Location of three simulated public spaces and aerial view of the respective urban zones. Source: CAOP and Google Earth Pro imagery, © Maxar Technologies.

4.2. Scenario Design

This study explored a range of adaptation strategies for outdoor public spaces aimed at improving thermal comfort and catering to the specific needs of the older population. Using the ENVI-met simulation model, different scenarios were developed and analysed to predict their impacts on microclimate conditions and overall OTC.

The tested adaptation strategies were informed by both the existing literature and on-site observations. Observational data revealed that older people frequently engaged in outdoor activities such as walking, socialising, playing chess, and resting on shaded benches. The strong preference for seating areas highlights the growing importance of accessible resting points for older adults as part of their daily outdoor routines [58]. These findings underscore the pivotal role of seating in facilitating mobility and social participation among older users in outdoor public spaces, aligning with previous research that identified seating as a crucial factor in promoting active and inclusive ageing in outdoor environments [59].

Furthermore, within the scope of the CAOP project, through its participatory methodological approach, older residents were actively involved by means of in-depth interviews, go-along interviews, and emotional mapping, in addition to observing public space users. Focusing on climate adversities, the older residents expressed their difficulties while using the outdoor public spaces and transmitted their preferences and suggestions [58].

The tested adaptation strategies, focused on enhancing outdoor comfort through modifications related to vegetation, shading, seating points, and pavement materials, with particular attention to the identified needs of older residents, were the following:

- Adaptation Strategy 1 involved the expansion of grass-covered surfaces and the introduction of additional vegetation to promote natural cooling through shading and evapotranspiration.
- Adaptation Strategy 2 incorporated the installation of shading structures, such as pergolas, combined with the inclusion of seating areas strategically placed along pedestrian walkways to provide rest and shelter from direct sunlight.

- Adaptation Strategy 3 focused on replacing existing pavement materials with cool materials, designed to reflect more solar radiation and reduce surface heat accumulation.

Figures 5–7 visually illustrate the spatial implementation of these three adaptation strategies across the studied public spaces (PS) in the selected zones.

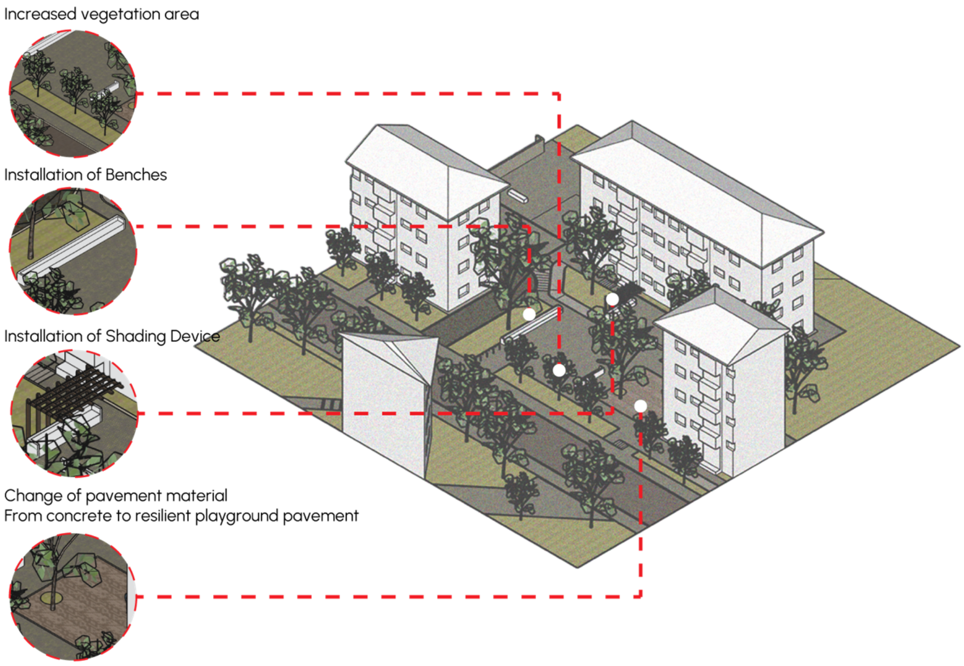

Figure 5. 3D model representing adaptation strategies for PS1.

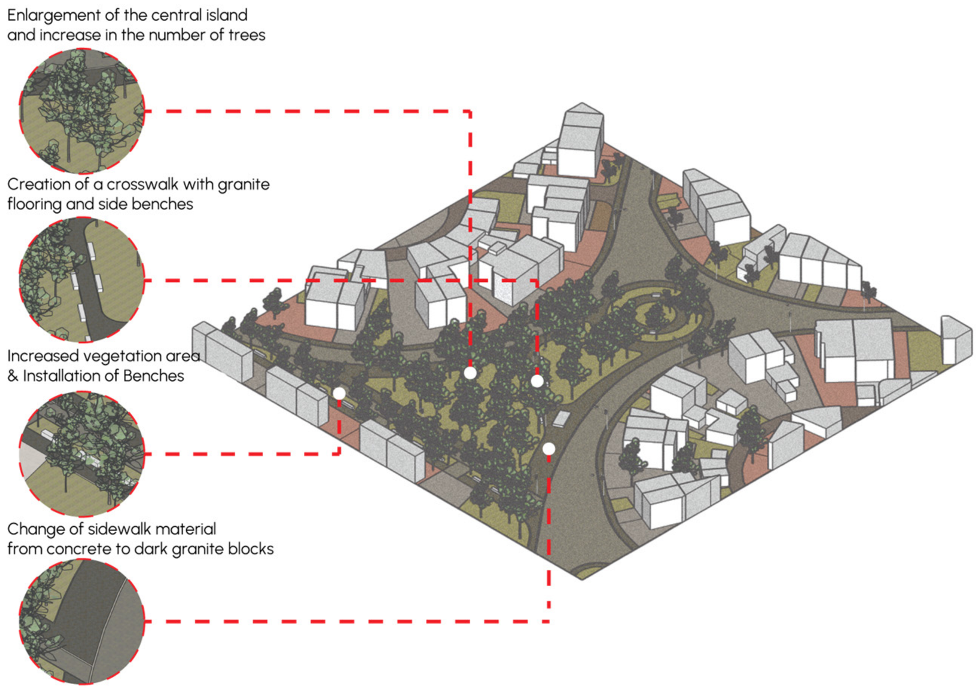

Figure 6. 3D model representing adaptation strategies for PS2.

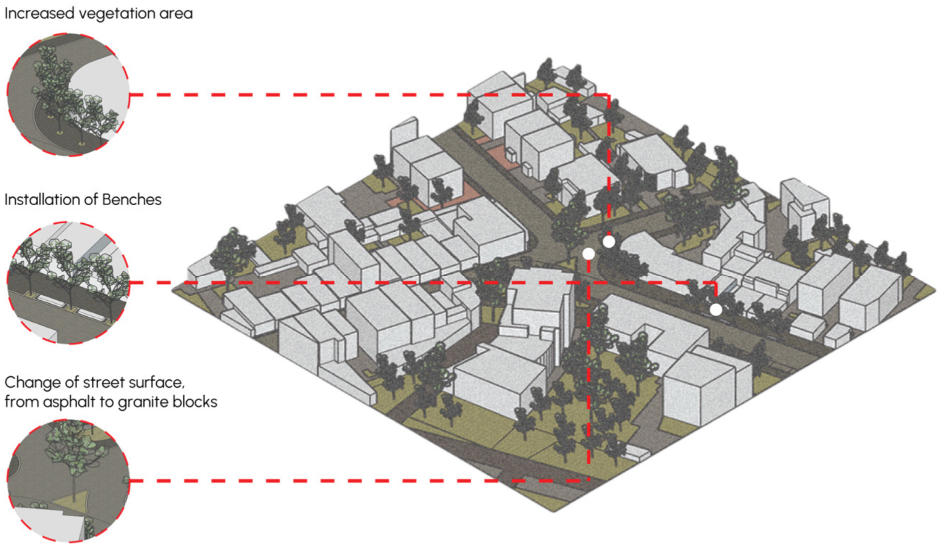

Figure 7. 3D model representing adaptation strategies for PS3.

4.3. Model Configuration

Since the primary focus was on studying the impact of some modifications on outdoor microclimate and thermal comfort, several numerical simulations were performed using ENVI-met V5.7.2, a validated three-dimensional microclimate modelling system [38,60–62].

Executing an ENVI-met simulation necessitates the definition of three primary data structures: the Area Input file, the Database, and the Configuration file [60]. The Area Input file (.INX) establishes the domain's spatial resolution and the properties of the orthogonal 3D calculation mesh, allowing for user-defined equidistant or telescoping grids across the x, y, and z axes. Integration with the Database ensures that descriptive parameters (such as albedo, thermal conductivity, water content, etc.) for soil, vegetation, and surface materials can be utilised to resolve the mathematical model's governing equations. Finally, the Configuration/Simulation file (.SIMX) prescribes the simulation's operational parameters, including the initial and boundary meteorological conditions.

This study employed an integrated 3D visualisation research method that utilises a combination of SketchUp, the ENVI-met INX plugin, and the core ENVI-met software. The foundational input data for microclimatic modelling was established within the SketchUp Environment, a platform favoured by designers and engineers for its comprehensive 3d modelling features. The crucial step of converting the raw 3d geometry (including building configurations, terrain, and vegetation) into the required ENVI-met input formats, specifically the area input file (.INX), is facilitated by the ENVI-met INX plugin. This specialised tool, developed by Antonello Di Nunzio, automatically generates the necessary files for each simulation iteration. This approach was chosen for its flexibility and efficiency, as it allows for quick modifications to building materials or shapes without requiring a rebuild of the model from scratch. The use of the ENVI-met INX plugin was specifically designed to address certain limitations inherent in the standard ENVI-met software for microscale simulations and to enhance its integration capabilities with external modelling tools. Vegetation data used in the models were sourced from an open-source GIS file provided by the Municipality of Porto, ensuring the use of authoritative local data for biophysical inputs.

To analyse the effects of various adaptation strategies, six models were simulated and then compared, as illustrated in Figure 8.

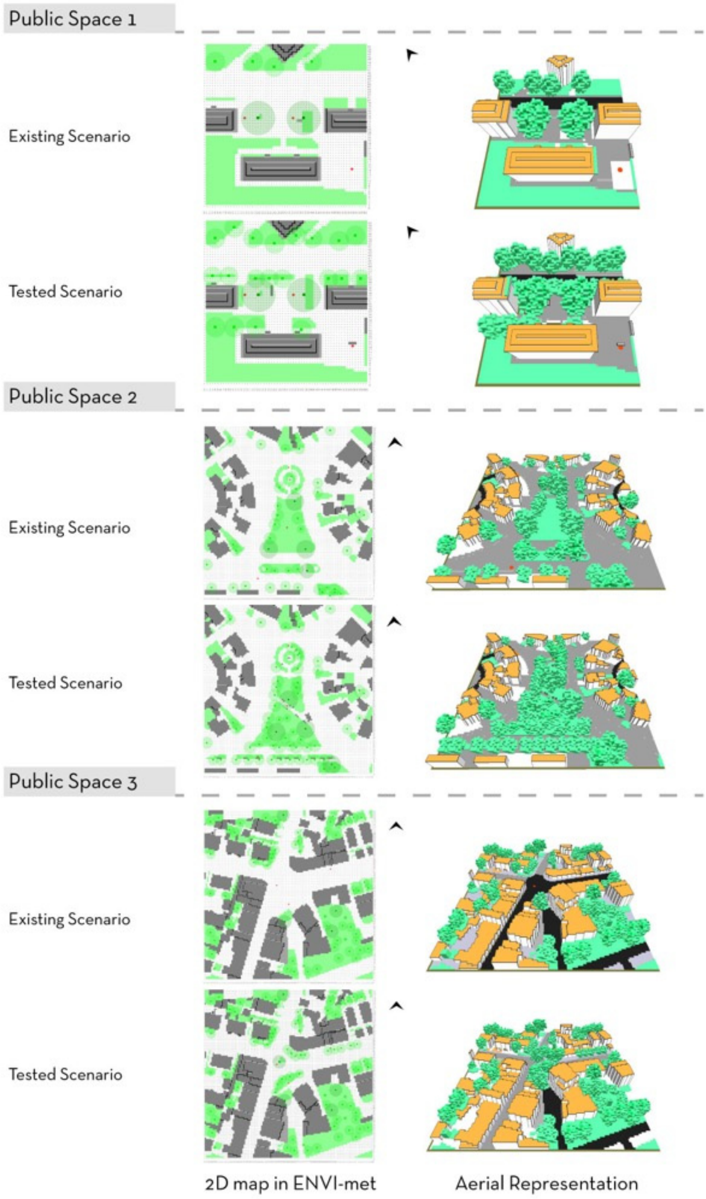

Figure 8. ENVI-met model of the case studies.

4.4. Study Time, Climate Data and Physical Properties of Materials and Vegetation

The study was conducted during the summer season, a critical period for outdoor comfort conditions in areas with an intense UHI effect. Climate change predictions for Porto point to a significant increase in the frequency and intensity of heatwaves. The number of very hot days, with temperatures exceeding 35 °C, and tropical nights, with minimum temperatures of 20 °C, is also expected to increase.

Given these predictions, the simulations were performed for the hottest day (the 10th of August) of a climate reference year in Porto (Typical Meteorological Year for Porto, derived from a statistical standard procedure applied to long-term climatic records provided through the national meteorological dataset), with climate data that included hourly values of air temperature, specific humidity, direct and diffuse solar radiation, wind speed, and wind direction (Figure 9). The purpose of selecting the hottest day was to evaluate peak heat-stress conditions, which are most critical for vulnerable older populations. The main objective was to compare the Existing Scenario (ES) vs. the Tested Scenario (TS) under identical meteorological conditions.

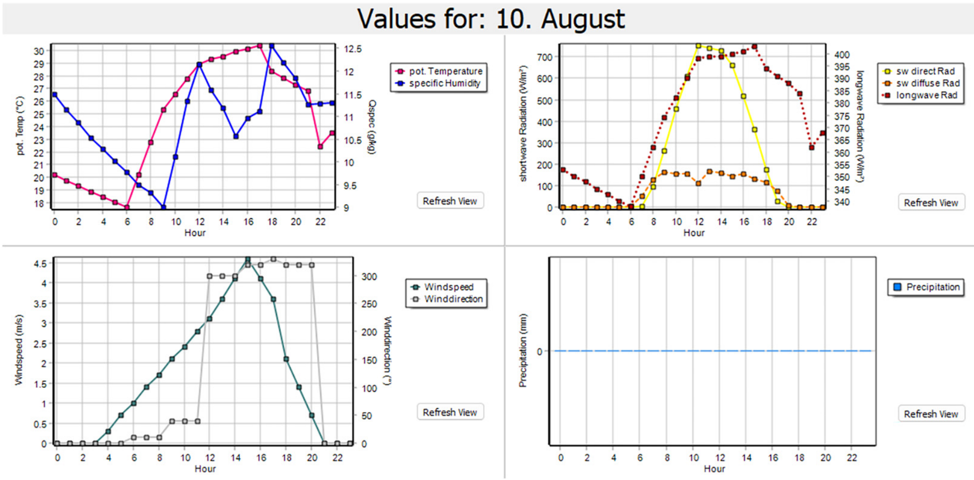

Figure 9. Porto meteorological data of the reference year's hottest day (10 August).

It is essential to note when interpreting the results that even the hottest day of the reference year presents less demanding conditions than the predicted hot days ahead. The research was based on a 24-h simulation.

Tables 2–4 provide the values of the physical properties of the materials used in the simulations.

The trees added to the model were consistent with the planted species, including *Acer campestre*, *Acer Pseudoplatanus*, *Quercus rubra*, *Aesculus hippocastanum*, and *Malus domestica* (Table 5).

Table 2. Physical properties of the soil materials used in the ENVI-met model.

Physical Properties	Soil Materials		
	Default Soil Profile Underneath a Building	Sandy Loam	Loamy Soil
Roughness	0.010	0.015	0.015
Albedo	0.200	0.200	0.000
Emissivity	0.900	0.900	0.900

Table 3. Physical properties of the wall materials used in the ENVI-met model.

Physical Properties	Wall & Roof Materials		
	Brick Wall (No Insulation)	Concrete Wall (Cast Dense)	Roofing Tile
Thickness (m)	0.30	0.30	0.05
Absorption	0.70	0.70	0.70
Transmission	0.00	0.00	0.00
Reflection	0.30	0.30	0.30
Emissivity	0.93	0.94	0.93
Specific Heat (J/kg·K)	900	840	800
Thermal Conductivity (W/mK)	0.64	1.90	0.84
Density (kg/m^3)	1500	2500	1900

Table 4. Physical properties of the pavement materials used in the ENVI-met model.

Physical Properties	Pavement Materials						
	Granite (Single Stones)	Dark Granite	Asphalt	Concrete (Dark)	Concrete (Gray)	Concrete (Light)	Styrene Butadiene Rubber
Roughness	0.010	0.010	0.010	0.010	0.010	0.010	0.003
Albedo	0.350	0.250	0.120	0.200	0.300	0.500	0.100
Emissivity	0.900	0.900	0.900	0.900	0.900	0.900	0.900

Table 5. Physical properties of the vegetations used in the ENVI-met model.

3D Plant Species	Simulation Tree Scenarios	Values
Sycamore Maple (*Acer Pseudoplatanus*)	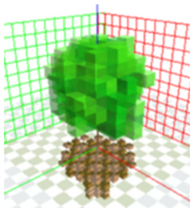	Height (m): 8.89 Width (m): 6.67 × 6.67 LAD (August): 1.00 Number of cells: 13 × 13 × 10 Foliage Shortwave Albedo: 0.18 Foliage Shortwave Transmittance: 0.30
Field Maple (*Acer Campestre*)	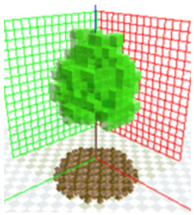	Height (m): 14.75 Width (m): 8.29 × 8.89 LAD (August): 1.00 Number of cells: 15 × 15 × 16 Foliage Shortwave Albedo: 0.18 Foliage Shortwave Transmittance: 0.30
Red Oak (*Quercus Rubra*)	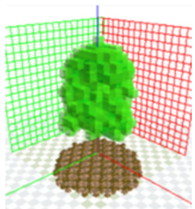	Height (m): 14.44 Width (m): 9.37 × 10.41 LAD (August): 1.00 Number of cells: 17 × 17 × 16 Foliage Shortwave Albedo: 0.18 Foliage Shortwave Transmittance: 0.30
Horse Chestnut (*Aesculus Hippocastanum*)	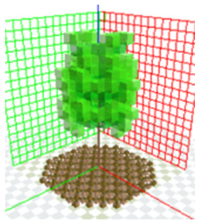	Height (m): 14.92 Width (m): 18.26 × 8.20 LAD (August): 1.00 Number of cells: 15 × 15 × 16 Foliage Shortwave Albedo: 0.18 Foliage Shortwave Transmittance: 0.30
Apple Tree (*Malus Domestica*)	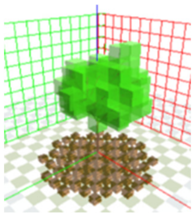	Height (m): 7.24 Width (m): 5.46 × 5.92 LAD (August): 1.00 Number of cells: 13 × 13 × 9 Foliage Shortwave Albedo: 0.18 Foliage Shortwave Transmittance: 0.30

5. Main Results and Discussion

The following sections present the main results of the microclimate simulations for all of the selected public spaces. The simulation's main results include microclimate variables such as Ta (°C), MRT (°C), RH (%), Ws (m/s), and Ts (°C).

https://doi.org/10.3390/urbansci10050249

Maps showing the spatial distribution of those variables were created using the LEONARDO software, integrated in ENVI-met. Buildings footprints are shown in black, while the results of the simulated microclimate variables are displayed using colour-coded ranges.

The maps in Figures 10–14 illustrate the spatial distribution of microclimate variables at 14:00, for the three simulated outdoor public spaces under two scenarios:

- Existing Scenario (current urban form);
- Tested Scenario (modified urban form with design interventions).

5.1. Comparison of the Microclimate Variables

5.1.1. Air Temperature (Ta)

The simulated potential Ta maps (Figure 10) revealed how the spatial configuration and vegetation arrangement influenced microclimatic performance across the three public spaces. The tested scenarios generally showed a reduction in high-temperature zones and a slight increase in cooler surfaces, suggesting that the tested interventions (adding greenery, shading, and reducing or changing paved surfaces) mitigate heat buildup, with effects on the Ta.

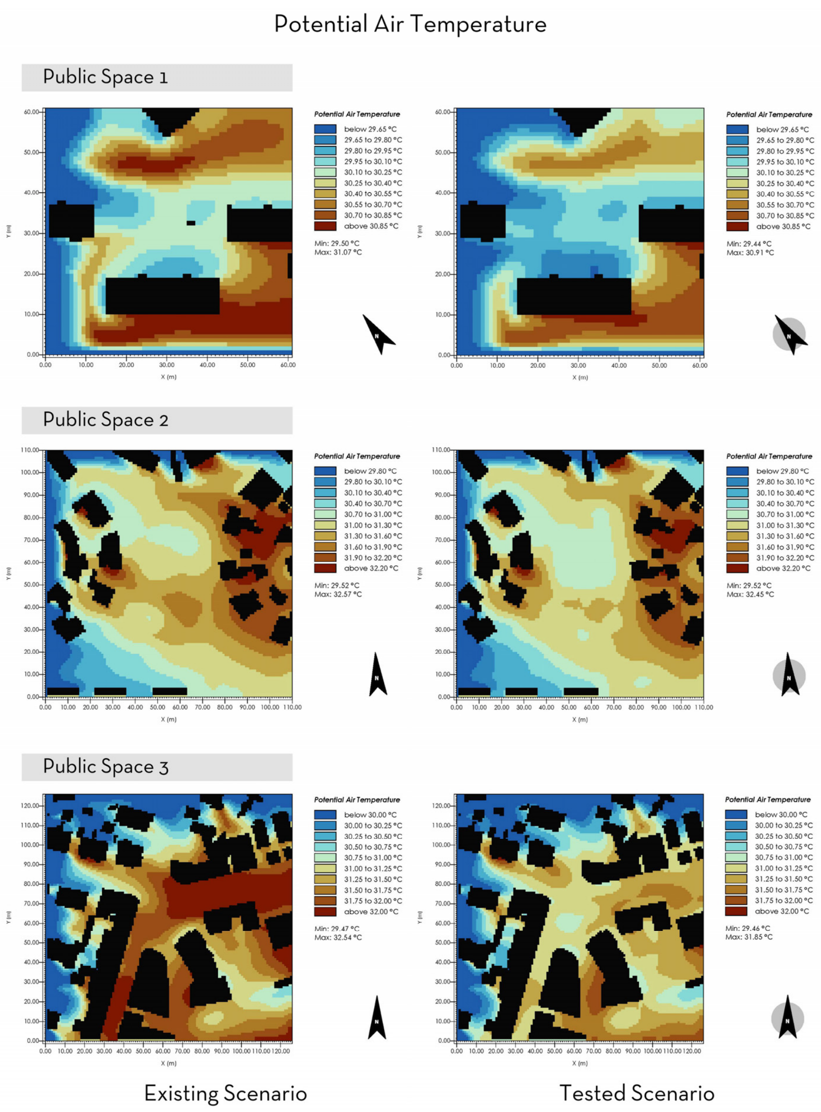

Figure 10. Spatial distribution of Ta at 1.5 m height, at 14:00. Cooler zones (blue) indicate lower Ta values and improved thermal comfort, whereas warmer zones (orange to brown) denote heat accumulation around built surfaces. Built forms are represented in black.

In PS 1, the existing scenario exhibited elevated Ta values (≈30–31 °C) concentrated near the southern and central building blocks, while peripheral zones remained relatively cooler. This reflects the combined effect of extensive impervious surfaces and high solar exposure. In the tested scenario, additional vegetation and tree canopy coverage visibly moderated the Ta values, expanding the cooler zones (≈29–30 °C) and reducing hot spots around the buildings, particularly near the newly added grass-covered surfaces and trees. This cooling effect can be attributed to evapotranspiration. Though the temperature drop was small (generally less than 0.5 °C), the smoother temperature gradient suggests improved ventilation and shading efficiency, particularly near the central courtyard.

In PS 2, in the existing scenario, cooler conditions already appeared around the green central space, while the circular arrangement of buildings created a heat pocket in the eastern zone due to reduced airflow and exposure to solar radiation, reaching about 32.6 °C. In the tested scenario, the reinforced vegetation and the addition of grass surfaces around the central island produced a noticeable cooling effect. This was visible as expanded cooler zones radiating outside from the core. The maximum Ta slightly decreased (≈0.5–0.9 °C) in adjacent pathways and open segments. This can also be attributed to the change in pavement material around the central green space. However, warm pockets still persisted in the eastern zone since the street geometry limits ventilation, and shading remains limited.

In PS 3, the dense urban layout created several high-temperature clusters, with Ta values reaching approximately 31–32.5 °C along street corridors and between building blocks towards the southern and eastern sides. This heat retention is primarily due to the limited vegetation and highly impermeable, low-albedo surfaces. This also reflects the canyon's low sky view factor, high heat storage in both vertical and horizontal surfaces, and restricted airflow. The tested scenario introduced additional trees and vegetation pockets along the streets and courtyards, resulting in a noticeable cooling effect on the air. Additionally, the change in street surface material from asphalt to granite blocks contributed to a reduction in surface heat uptake. However, the canyon geometry dominated the thermal signature, since radiation emitted by the building façade and solar radiation overshadowed the benefits of surface reflectance improvements.

The maps show that the highest Ta values occurred over asphalt and sidewalks, while the lowest Ta values were observed over grass surfaces, under trees, and in other shaded areas, including those shadowed by buildings and in the shade of trees. The simulated scenarios indicate that incorporating green areas can lower the Ta, particularly in the early afternoon, when solar radiation is strongest, and surfaces have warmed up over the preceding hours. While the changes in Ta were modest, the tested scenarios across all three sites clearly demonstrated the microclimatic benefits of the combined effect of vegetation-based interventions and high-albedo pavement materials, creating micro-scale cooling patterns.

5.1.2. Mean Radiant Temperature (MRT)

MRT maps (Figure 11) provide a measure of thermal stress influenced by solar radiation, surface reflectivity, and shading from buildings or vegetation. Across all three public spaces, the tested scenarios demonstrated a noticeable reduction in high-radiation zones, particularly in open and paved areas.

In PS 1, the existing scenario revealed elevated MRT values (≈60–70 °C) around open, exposed surfaces near the southern façades and in paved areas. These exposed surfaces absorb solar radiation and re-radiate it to the surrounding environment, amplifying the heat stress. Cooler zones (≈38–46 °C) were primarily found in shaded areas along building edges. In the tested scenario, increased tree cover and ground-level vegetation expanded these shaded areas, reducing radiant heat intensity, particularly in the central plaza. The overall temperature field became more balanced, showing a clear shift from large, homogeneous red/pink zones (hot) to fragmented cooler MRT patches. This improvement demonstrates the cooling role of canopy shading and reduced surface radiation absorption.

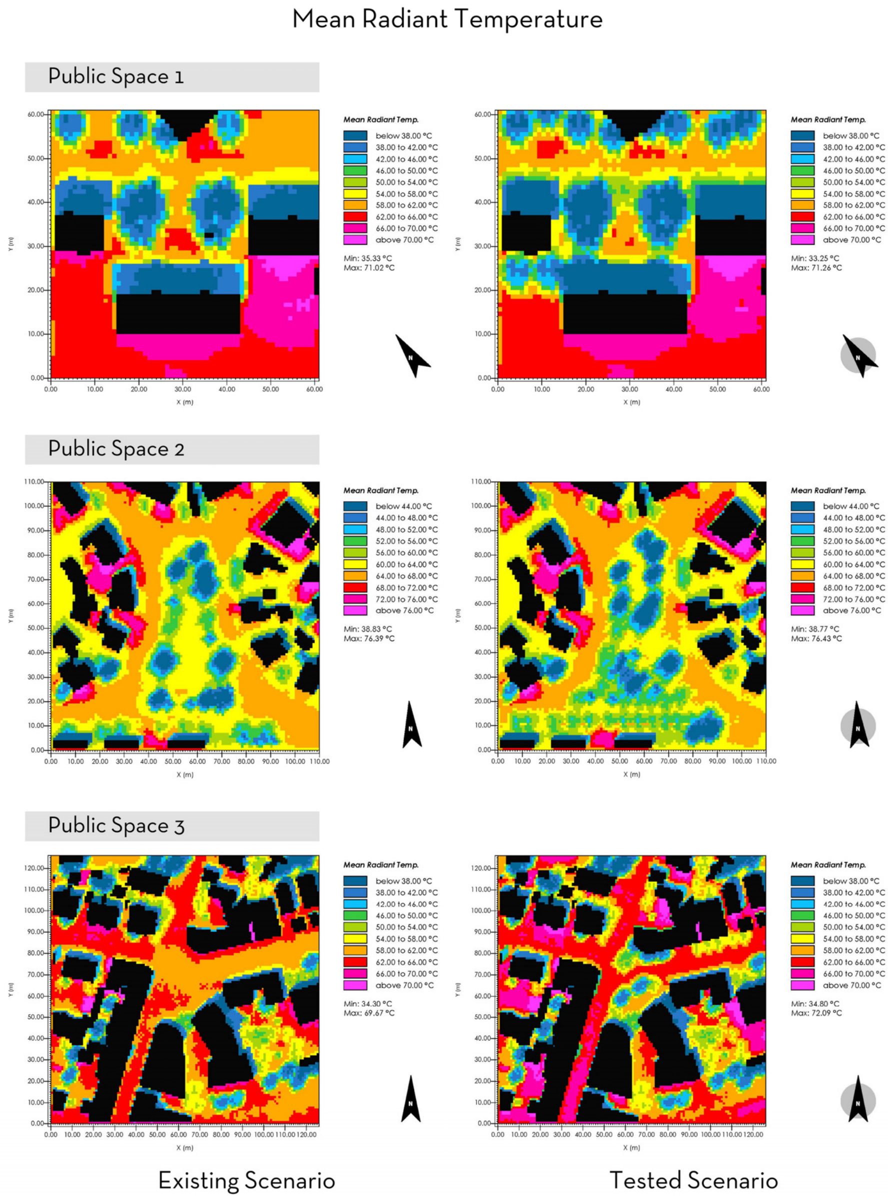

Figure 11. Spatial distribution of MRT at 1.5 m height, at 14:00. Cooler zones (blue) indicate lower radiation exposure and higher shading effectiveness, while warmer zones (red to purple) represent areas of higher radiant heat accumulation due to solar exposure and surface reflection. Built forms are represented in black.

PS 2 exhibited a highly heterogeneous MRT pattern in the existing scenario, resulting from the interplay of vegetation, paved areas, and irregular building orientations. High MRT values predominated in exposed areas, particularly near building corners and asphalt streets, whereas the central green space exhibited lower MRT due to partial shading. The tested scenario introduced dense vegetation and tree canopies throughout the central green space, visibly lowering the MRT levels (down to ≈56–60 °C) and creating broader, cooler patches across the inner green area. However, peripheral built-up zones remained relatively warm due to limited shadow penetration.

PS 3 exhibited the most extreme existing MRT conditions. The street canyon morphology, with narrow sidewalks, increased the absorption and reflection of solar energy. As a result, MRT values peaked and remained consistently high throughout the canyon (often exceeding 70 °C), regardless of localised shade. In the tested scenario, the addition of street trees, pocket greenery, and shading structures resulted in small localised MRT reductions; however, the canyon geometry limits further improvement. The cooling pattern was most pronounced where vegetation was strategically positioned to intercept direct solar gain. In some segments, MRT increased slightly due to reflected radiation from the introduced high-albedo surfaces, illustrating the complexity of radiative behaviour in narrow spaces.

The simulation results demonstrate how this parameter changes at the pedestrian level (1.5 m) across scenarios. Greater differences were observed between sunny and shaded areas, with maximum values recorded on paved surfaces. For the tested scenarios, trees primarily provided solar radiation shielding, preventing direct shortwave radiation. Conversely, the change of the pavement material to a more reflective one increased the MRT along the street canyon.

5.1.3. Relative Humidity (RH)

RH maps (Figure 12) showed minor but consistent increases across all areas in the tested scenarios. These changes demonstrate the influence of vegetation density and surface permeability in enhancing local evaporative cooling. Overall, the tested configurations exhibited slightly higher RH, particularly around green and shaded zones, aligning with the reductions in potential Ta and MRT observed previously.

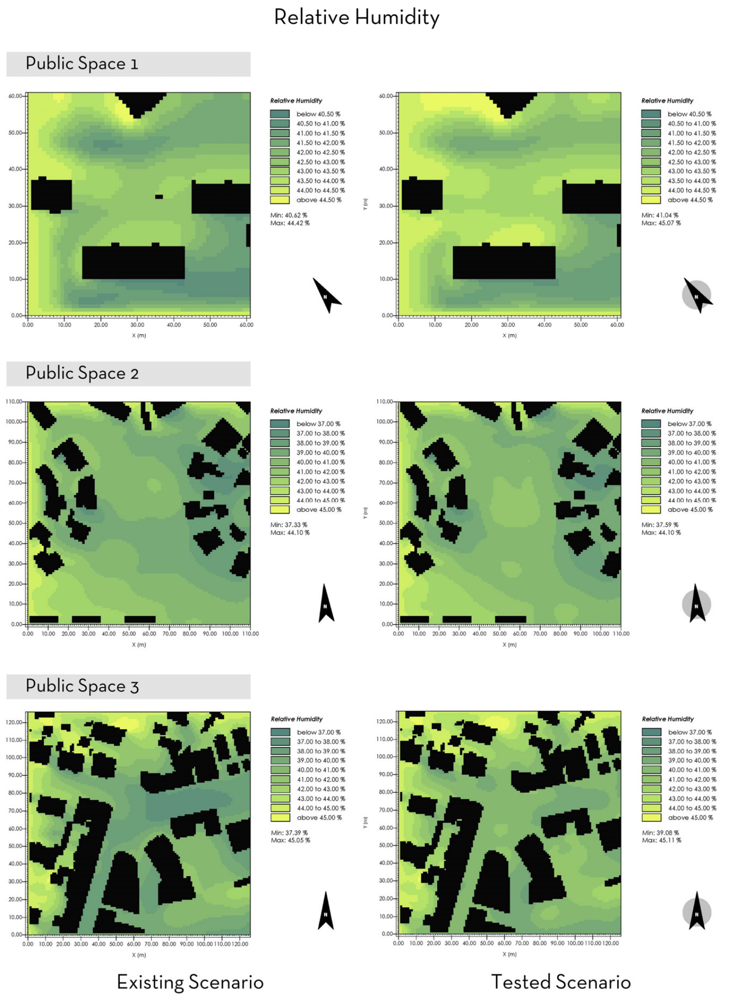

Figure 12. Spatial distribution of RH at 1.5 m height, at 14:00. Higher values (yellow tones) indicate more humid and thermally comfortable microclimates, while lower values (green tones) represent drier and warmer air conditions. Built forms are represented in black.

PS 1 exhibited moderate humidity levels (≈42–43%) in the existing scenario, with drier zones adjacent to exposed paved surfaces. In the tested scenario, added vegetation and increased canopy coverage raised the RH slightly (≈44–45%), producing a more uniform humidity field. The enhancement was most noticeable near the central and northern green zones, suggesting improved microclimatic moisture retention due to evapotranspiration.

The existing scenario in PS 2 revealed an RH around 37–40%, with the central green space appearing relatively dry. In the tested scenario, expanded tree canopy and vegetation coverage in the central space led to a localised rise in RH (≈41–43%), particularly along shaded edges. Although the circular morphology still limits ventilation, the central vegetated space acts as a localised moisture reservoir, improving comfort for pedestrians and particularly benefiting older individuals by maintaining slightly more humid and therefore less dehydrating conditions in the central node.

PS 3, with its dense urban form and narrow streets, exhibited relatively low RH (≈37–38%) in its existing condition, particularly along built-up corridors. The tested scenario introduced street trees and vegetated courtyards, contributing to a slight increase in humidity (≈38–40%) and a more balanced distribution across the site. The enhancement was most evident near vegetated intersections, where microclimatic shading and reduced radiant heat strengthened local moisture retention.

Across all three sites, the tested scenarios indicated slight but consistent increases in RH, which complements the observed cooling effects in air and radiant temperatures. The results highlight the synergistic role of vegetation in enhancing both cooling and moisture balance through the process of evapotranspiration. The degree of improvement correlated with the vegetation density and openness of each site: PS 1 achieved the most uniform humidity field, PS 2 showed localised improvement in the central zone, and PS 3 benefited from enhanced street-level moisture retention despite its compact morphology.

5.1.4. Wind Speed (Ws)

Ws maps (Figure 13) illustrate how urban morphology and vegetation can affect local airflow patterns. In the three areas studied, the Ws simulations showed little variation throughout the day. However, the differences between the existing and tested scenarios were subtle yet meaningful. In all time periods, lower Ws values were detected near buildings, while open areas exposed to the prevailing wind experienced higher Ws values.

In PS 1, the existing scenario exhibited moderate airflow (≈2.5–3.5 m/s) across the open areas, with slight stagnation zones developing near the building facades due to wake effects. In the tested scenario, the introduction of additional trees and ground vegetation resulted in a slight reduction in Ws within the central plaza. While these changes do not entirely obstruct ventilation, this effect is compensated for by the shading from tree canopies.

In the existing scenario, PS 2 exhibited higher Ws along the main connecting roads, while the inner streets exhibited stagnant or low-wind zones due to limited throughflow and shielding by buildings. The central green space showed moderate air flow. The tested scenario, featuring additional tree canopy and permeable surfaces, yielded a slightly reduced wind intensity in the core zone while improving directional flow along the periphery. The vegetation acts as a natural buffer, softening wind gusts without completely obstructing movement. However, the weak ventilation in the inner streets persists, resulting in pockets of stagnant warm air. The overall effect is a more uniform and comfortable airflow in the central area, making it more inviting for older adults seeking resting points.

PS 3, characterised by dense buildings and street canyon morphology, displayed the lowest Ws (≈0.8–1.2 m/s) along the axis of São Roque da Lameira street in both scenarios. However, we observed moderate airflow along the secondary street that intersects it. In

https://doi.org/10.3390/urbansci10050249

the tested scenario, the addition of street-level greenery and open corridors resulted in minor improvements in cross-ventilation, particularly along the east–west–oriented street. However, unlike open spaces, the canyon lacks the capacity for improved cross-ventilation, meaning that wind cannot effectively disperse the accumulated radiant heat. Nonetheless, the modifications help reduce localised heat buildup while maintaining adequate comfort in shaded pedestrian zones. Finally, several stagnation pockets observed near the buildings remained relatively unchanged.

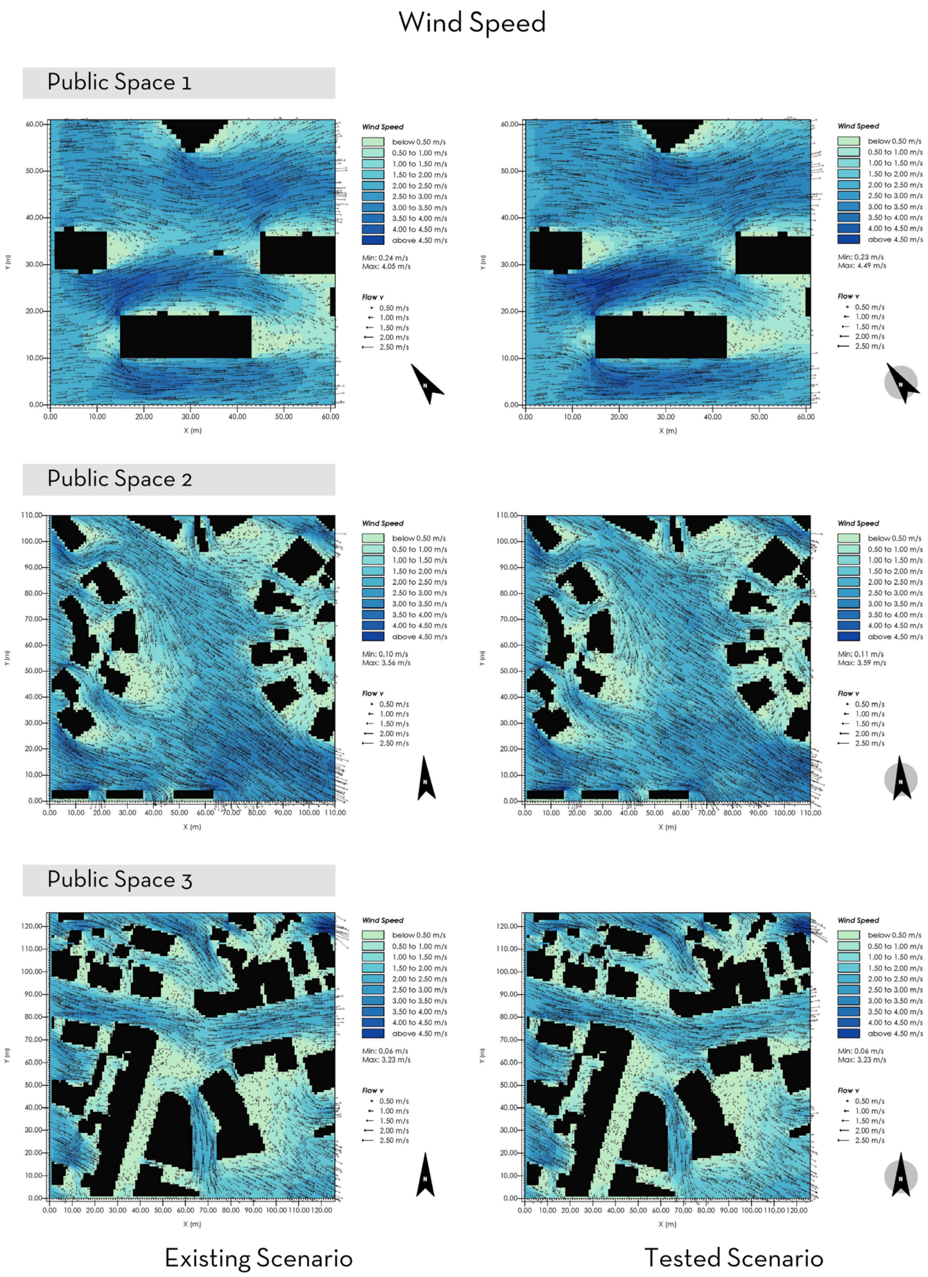

Figure 13. Spatial distribution of Ws at 1.5 m height, at 14:00. Higher Ws values (blue) represent enhanced ventilation and cooling potential, while lower speeds (cyan) indicate sheltered or stagnated airflow zones around built-up areas. Built forms are represented in black.

The tested scenarios in all three areas revealed minor reductions in average Ws due to increased vegetation, but this effect was compensated for by shading.

5.1.5. Surface Temperature (Ts)

Ts maps (Figure 14) revealed clear spatial variations influenced by solar exposure, land cover type, material properties, and shading patterns. Across all three study areas, the tested scenarios exhibited lower Ts values.

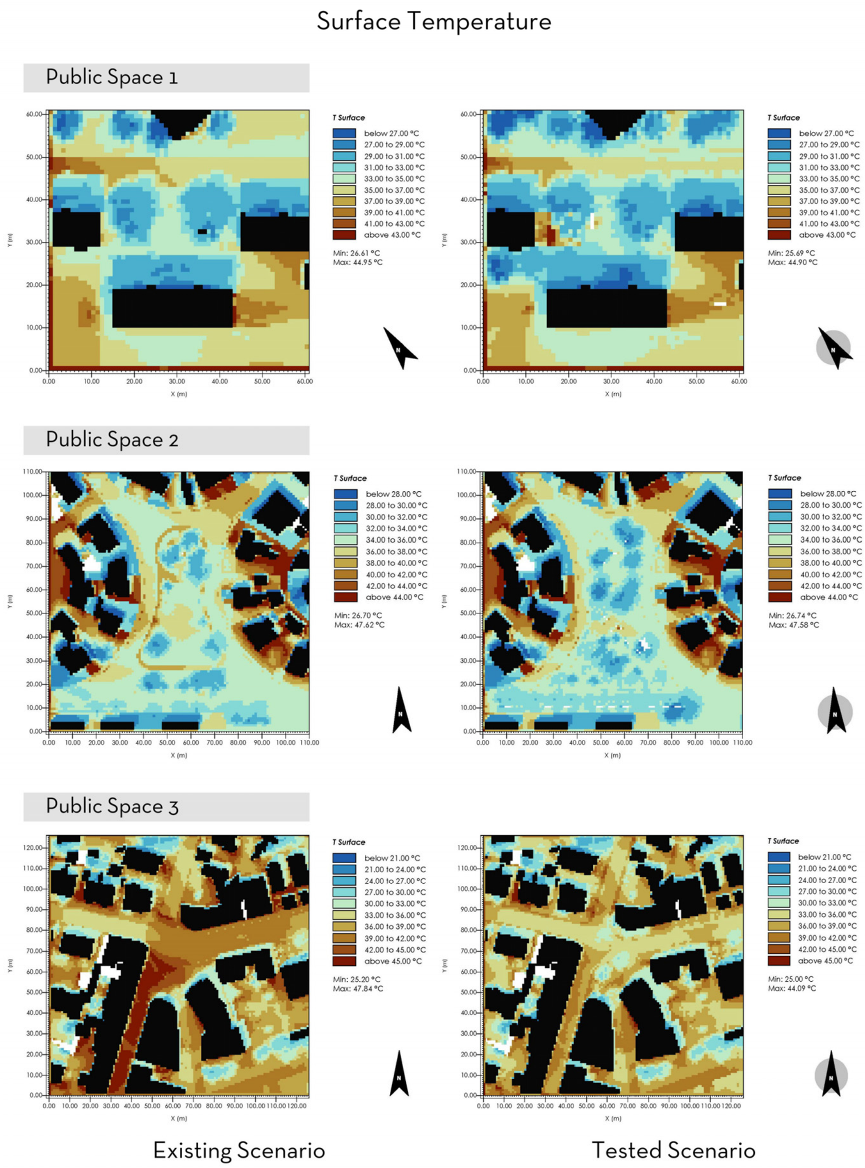

Figure 14. Spatial distribution of Ts, at 14:00. Cooler zones (blue) represent lower Ts values associated with vegetation and shaded areas, while warmer tones (yellow to brown) indicate heat accumulation on impervious or sun-exposed surfaces. Built forms are represented in black.

PS 1 exhibited elevated Ts values (≈41–45 °C) in the existing scenario, particularly over paved and exposed surfaces near buildings. In the tested scenario, the addition of tree cover and vegetated ground surfaces reduced these high-temperature zones, producing cooler patches (≈35–40 °C) around central open areas. The more extensive blue regions highlight improved surface shading and lower heat storage on pavements, indicating effective thermal mitigation through landscape design.

It must be noted, however, that the change in the pavement covering material in a small area on the northwest side of the central area, close to the building on the left in the map, increased its Ts. In this case, the change was carried out for a functional reason, creating a resilient pavement for a small playground. The increase in Ts was expected since, as shown in Table 4, Styrene Butadiene Rubber, the chosen material, has a very low albedo. One possible solution for this issue would be to ensure the shading of that area.

The existing scenario in PS 2 exhibited strong heat accumulation (≈47 °C) in the paved areas near the buildings. The ring-shaped building arrangement restricts airflow, amplifying local heating on paved areas. In the tested scenario, the introduction of new vegetation in the central green space and along building edges cooled the core zone by approximately 2–3 °C. Additionally, the change in pavement materials from concrete to granite around the central green space showed reductions in Ts. The resulting pattern exhibited enhanced surface cooling and improved uniformity, highlighting the role of greenery in mitigating thermal concentration within semi-enclosed urban layouts.

PS 3 registered the highest Ts values (≈46–48 °C) under the existing scenario, concentrated along roadways and pavements with minimal vegetation. In the tested configuration, the inclusion of street trees and small vegetation patches produced localised Ts reductions, particularly along pedestrian routes. The change in pavement material on São Roque da Lameira street to a material with a higher albedo resulted in a clear reduction in Ts, as expected. The changes demonstrate a notable improvement in surface cooling and reduced heat storage.

Among the three sites, PS 3 benefited the most due to the change in its previously high thermal load and limited greenery, followed by PS 1, where courtyard vegetation moderated surface heat, and PS 2, which showed moderate improvement within its enclosed morphology.

5.2. Comparison of Physiological Equivalent Temperature

Physiological Equivalent Temperature (PET) is the most integrative indicator in this study because it synthesises the previous variables, transforming them into an interpretable index of heat stress. To assess thermal comfort conditions for different demographic groups in the studied public spaces, two distinct individual profiles were defined in the PET simulations (Table 6), an active age adult (male) and an older adult (female). A 35-year-old male individual was selected to represent the active-age adult. Older females aged 80 were selected to represent the demographic group of older individuals aged 66 and above, which constituted the most significant demographic segment in the selected study areas. This allowed the simulations to illustrate variations in thermophysical responses between an active-age individual and an older, more vulnerable individual. Like the microclimate variables, the Physiological Equivalent Temperature (PET) output (Figure 15) was based on data from August 10 of the reference year.

Table 6. Individual person settings for PET calculation.

		Active Age Adult	**Older Adult**
Body Parameters	Age of Person	35 yr	80 yr
	Biological Gender	Male	Female
	Height (m)	1.75	1.65
	Weight (kg)	75	65
Clothing Parameter	Static Insulation Outdoor (clo)	0.5	0.5
	Static Insulation Indoor (clo)	0.9	0.9
Personal Metabolism	Total Metabolic Rate (W)	164.49	137.02

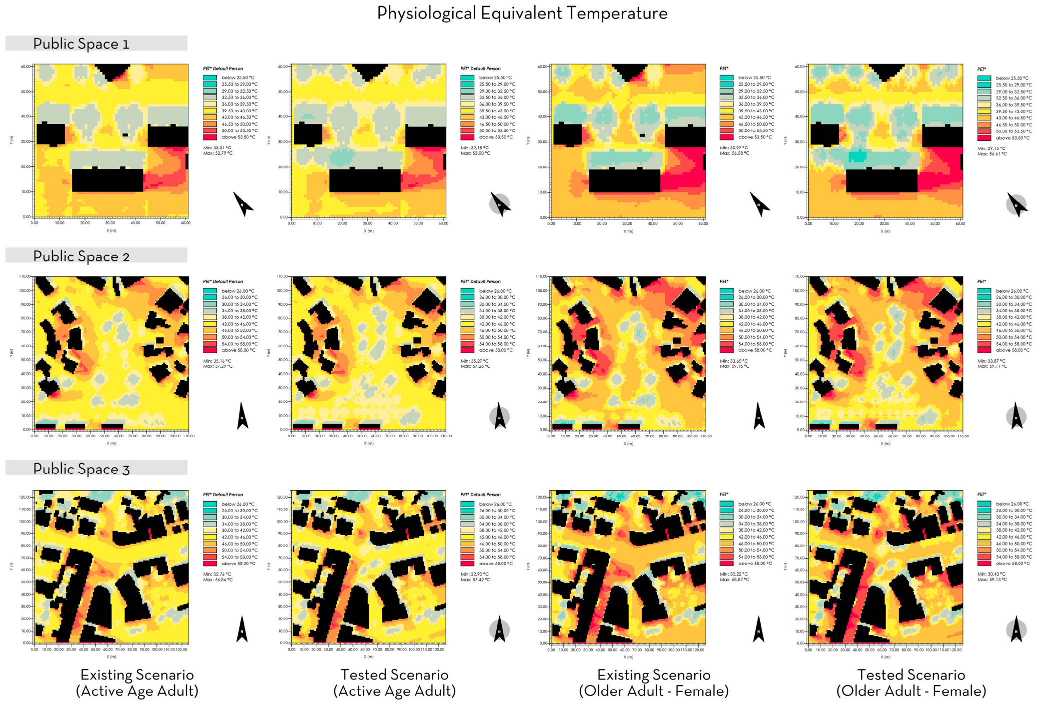

Figure 15. Spatial distribution of PET at 1.5 m height, at 14:00. Lower PET values (cyan) indicate improved OTC, while higher values (red) reflect increased thermal stress. Built forms are represented in black.

Across all three study areas, the tested scenarios consistently exhibited reduced PET values, indicating an improved thermal environment achieved through vegetation enhancement and increased shading. However, the PET maps clearly indicate that older adults experience higher thermal stress levels, even under the same microclimatic conditions, due to biological and behavioural factors.

In PS 1, the current situation revealed large areas of high PET values (≈38 to 45 °C for the active-age adult and ≈40 to 48 °C for the older adult), primarily driven by solar exposure and high MRT across the paved surfaces. The PET maps for the older person showed broader red and orange zones compared to the default person, illustrating a stronger physiological stress to radiant and surface heat. In the tested configuration, with the addition of trees and increased vegetated surfaces, we observed improved PET values. The comparison between maps demonstrates that while both groups benefit from the interventions, improvement is more spatially meaningful than numerically large.

PS 2 exhibited some of the highest PET values (active-age adults ≈40–47 °C, older adults ≈44–49 °C) around the buildings, indicating that the circular building layout produces localised thermal accumulation. The enclosed geometry restricts airflow, amplifying perceived heat stress. The central green space, however, presented substantially lower PET values for both groups (default persons, 32–36; older adults, slightly higher). In the tested scenario, the expansion of vegetation around the central node increased shading and evapotranspiration, thereby enlarging the cooler PET zone. This improvement was evident in both user profiles, but older adults continued to experience substantially greater heat stress, with visibly larger red and orange zones remaining compared to the default person.

PS 3 showed the most extreme PET conditions in both scenarios due to its street-canyon morphology. The existing scenario displayed a continuous high PET corridor (active-age adults, 42–50; older adults, 45–52) with very limited spatial variation. High MRT from exposed asphalt in the form of long-wave radiation dominated thermal stress. Under the tested scenario, the inclusion of street trees slightly lowered the PET values typically localised to small, shaded segments along sidewalks. However, since the canyon maintains strong radiative trapping, PET improvements remain limited for both user types. The PET map for the older person showed virtually unchanged thermal stress distribution, indicating that the small-scale interventions cannot overcome the canyon-driven energy balance. In the street canyon, some worsening of PET could even be observed after changing the pavement material to one with a higher albedo.

Across all three areas, the older adult profile showed consistently higher PET values (typically +2 to +5) and a noticeably larger proportion of heat stress zones compared to the active-age adult. While adaptation measures improved microclimatic conditions in all three spaces for both profiles, older adults continue to face higher thermal stress levels and require a more protective spatial configuration.

To assess the efficacy of interventions, a deeper analysis of PET values was conducted by examining strategic locations (Point A, B, and C) for each of the public spaces, as shown below (Figure 16).

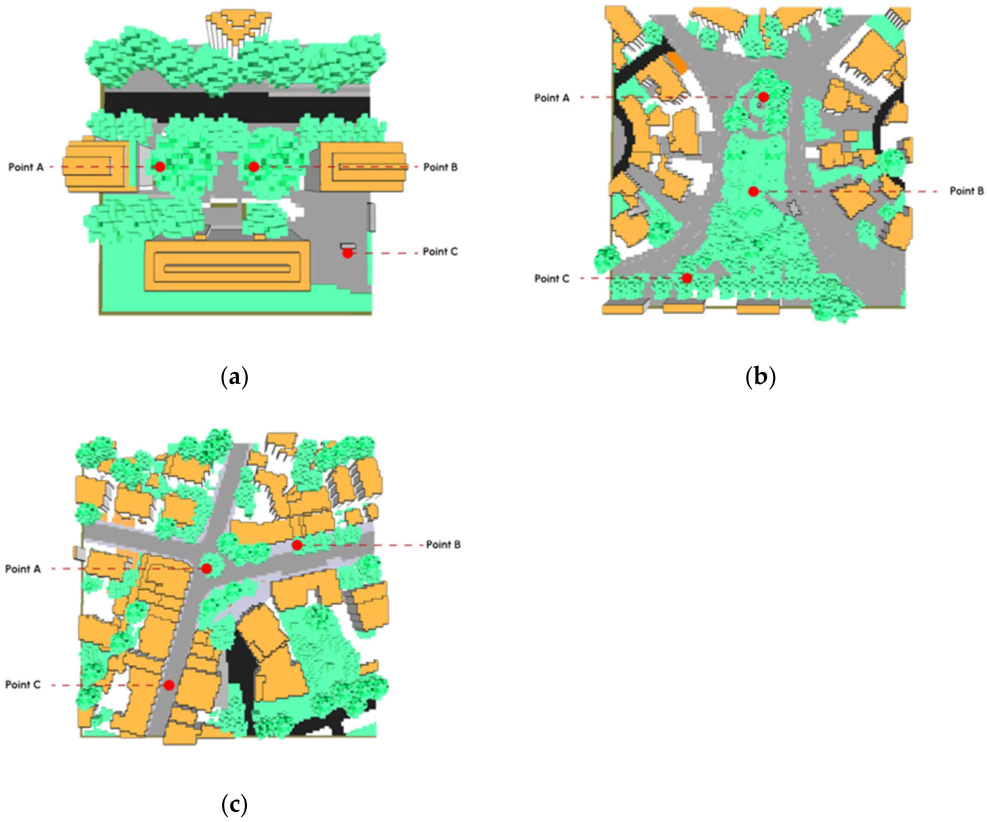

Figure 16. Chosen points for PET comparison. PS1 (**a**), PS2 (**b**), and PS3 (**c**), respectively.

The PET time-series results (Figure 17) provide meaningful insight into how microclimatic variations translate into thermal stress across different spatial configurations and demographic profiles. Across all three public spaces, PET increased sharply during late morning and peaked between 13:00 and 16:00, corresponding to periods of intense solar radiation and elevated MRT. Similar to the PET maps, it was observed that older adults were systematically exposed to higher PET values than active-age adults, with differences ranging from 2 to 4 °C during midday hours. This disparity demonstrates the physiological constraints of ageing, including reduced thermoregulatory efficiency and heightened sensitivity to Ta and radiative heat loads.

Figure 17. Comparison of PET values, throughout the day, at different locations in each public space (ES = Existing Scenario; TS = Tested Scenario).

The comparison between the existing and tested scenarios indicates that adaptation strategies yielded varying levels of effectiveness. Older adults benefited from the implemented strategies, but due to their elevated baseline stress levels, they remained at higher risk even after intervention. While the tested scenario mitigated peak PET, the reductions were insufficient in high-intensity canyon areas, where PET values frequently exceeded the critical thresholds. After sunset, PET values dropped sharply due to the reduction in MRT and solar-driven surface heating. By 22:00, PET stabilised across all sites, typically falling between 23 and 27 °C in the existing scenario. During late-night and early morning hours (00:00–06:00), PET values plateaued at around 18–23 °C, indicating cooler atmospheric conditions and reduced metabolic heat stress.

The percentages in Figure 18 represent the proportion of the 24-h period spent in each PET band for each public space (PS 01 03) and each scenario (ES = Existing Scenario, TS = Tested Scenario).

The PET bands perceived as “Comfortable” and “Slightly warm” presented higher percentages across all of the tested scenarios when compared to the existing ones for both demographic groups. The >41 °C band was always higher for older adults than for younger adults. This confirms their greater vulnerability despite identical environmental conditions. However, in the tested scenarios, this band decreased for both demographic groups across all public spaces.

Figure 18. 24-h distribution of PET with percentile assessment.

5.3. Limitations and Further Potential Developments

Despite this study's findings, several areas for future development exist that could enhance urban microclimatic assessments and climate adaptation strategies. While ENVI-met has been proven to be a valuable tool for comparative microclimate evaluation, its simulation process is quite time-consuming. This limitation restricted the number of simulation periods and alternative scenarios that could be explored within the available timeframe. Additionally, the software has limitations in accurately replicating the geometric characteristics of urban areas and existing buildings. This constraint raises concerns about the degree of precision of the results, although it does not hinder comparative analysis. In this study, to balance the computational efficiency with spatial resolution (optimising the calculation time and maintaining a proper level of detail), a uniform grid cell size of 1 × 1 m was adopted. Given the model's inability to accurately represent sloping roof planes, the structures were modified to conform to align with ENVI-met's rectilinear grid requirements, thereby approximating their volume. Irregular geometries were also standardised and represented using square blocks. As the software continues to evolve, it is expected that future versions will enhance its capabilities for modelling realistic urban geometries, ultimately improving the accuracy of microclimate simulations.

This research primarily used PET as the only measure for evaluating OTC. Further studies might consider employing multiple thermal comfort indices to verify and cross-reference the findings. Different indices could provide diverse insights into thermal comfort, leading to a more thorough evaluation of the effectiveness of adaptation strategies. The range of adaptation strategies examined in this research was restrictive. Future investigations could explore a broader range of strategies, including modifications to building materials and façade designs, which could significantly influence microclimatic conditions and thermal comfort. For instance, incorporating green roofs, green walls, and various cool pavements could be beneficial.

This study highlights several opportunities for future research, all of which aim to improve urban microclimates and environmental conditions. By broadening the range of tested adaptation strategies, utilising advanced simulation tools, incorporating various thermal comfort indices, and employing sensors for the real-time collection of climatic data, urban designers and practitioners will gain access to more comprehensive data and insights. As this research is refined and expanded, significant progress can be achieved in tackling the complex challenges presented by climate change and urbanisation.

6. Conclusions

This study highlights the crucial role of urban microclimatic assessment through simulation in the adoption of climate-adaptive design strategies to promote resilient, liveable, and age-friendly outdoor environments. Focusing on the highly vulnerable neighbourhood of *São Roque da Lameira* in *Campanhã*, Porto, the research demonstrates that vulnerability is not solely climatic but also socio-spatial, showing how urban morphology, surface materials, and vegetation collectively influence OTC, particularly for older populations who are physiologically more sensitive to heat. Through simulations conducted on three distinct residential configurations, the study provided an in-depth comparison of pre- and post-intervention scenarios, revealing how urban form fundamentally shapes both microclimate and the potential success of adaptation measures. The findings confirm that ENVI-met serves as an effective tool for preliminary microclimatic assessment, offering detailed insights into local atmospheric dynamics encompassing Ta, solar radiation, humidity, and wind flow, parameters essential for understanding and evaluating OTC.

Across all areas, PET outcomes consistently revealed higher thermal stress for older adults, with more continuous heat-exposed zones compared to the default adult, underscoring their heightened vulnerability and the critical importance of designing thermally accessible, age-inclusive public spaces. The use of PET for assessing the OTC was particularly advantageous in this respect, as it integrates demographic-specific parameters such as age, gender, metabolic rate, and clothing insulation. This alignment of thermal comfort evaluation with the needs and limitations of older individuals supports the development of targeted, context-sensitive interventions that promote well-being and social inclusion.

The comparative evaluation of adaptation measures showed that strategies fall broadly into two categories: urban heat mitigation measures, which actively reduce environmental heat loads, and protective measures, which primarily shield users from thermal exposure. In line with nature-based solution trends, the expansion of green spaces and the addition of new vegetation consistently emerged as the most effective interventions for lowering Ts, reducing MRT, and improving overall thermal comfort. Their dual functionality, providing shading while simultaneously cooling the surrounding air through evapotranspiration, makes vegetation a cornerstone of climate-resilient design. High albedo pavement materials further mitigated some negative effects. These materials reduce the amount of solar energy absorbed during the day, thereby lowering Ts and Ta. However, they must be used carefully in narrow spaces where the presence of close vertical surfaces may have a negative impact, and the reflected solar radiation by the pavement, reaching those vertical surfaces, may increase the value of MRT and consequently increase discomfort.

https://doi.org/10.3390/urbansci10050249

In contrast, non-natural structures, such as seating areas like benches and shading structures like pergolas, provided protective effects, offering immediate comfort through shade and opportunities for rest. However, these elements did not substantially modify the wider atmospheric conditions. Their contribution is therefore more behavioural and experiential, supporting users, especially older adults, by creating thermally safer micro refuges without altering the overall thermal performance of the space.

Despite variations across the three study sites, a consistent pattern emerged. Adaptation efforts were most successful in open or moderately enclosed morphologies, whereas dense morphologies exhibited limited improvement due to radiative heat trapping and constrained ventilation. These findings underscore the importance of integrating urban form into early-stage climate adaptation planning and emphasise the utility of predictive simulation tools. Embedding microclimate modelling within the planning workflow enables evidence-based decision-making, supports efficient resource allocation, and reduces the risk of implementing ineffective interventions. As shown in this paper, the same strategy may work very well in a certain outdoor space but not so well or even detrimentally in another space of different geometry and/or physical features.

Given the accelerating challenges posed by climate change, the intensifying UHI effect, and rising ambient temperatures, it becomes imperative to integrate microclimatic analysis as an initial step in the urban design and planning process. Rather than treating adaptation as a reactive measure, planners and designers should employ predictive modelling tools to evaluate and compare the potential effectiveness of different design interventions before their implementation. This data-driven approach not only minimises the risk of investing in strategies that fail to deliver measurable outcomes but also promotes the efficient allocation of urban resources. By embedding microclimate simulations within the planning workflow, cities can transition towards evidence-based, climate-responsive design practices that foster thermal comfort, environmental sustainability, and social well-being, with particular benefits for vulnerable populations such as older people.

In conclusion, the integration of microclimatic assessment into urban planning is not merely advantageous but fundamental in responding to the challenges posed by climate change. The findings of this study underscore the importance of adopting a holistic urban design approach that accounts for both the micro- and macro-scale environmental effects of adaptation strategies. At the micro-scale, this includes streets, squares, buildings, roofs, pavements, shading, vegetation, and reflective materials; at the macro-scale, it encompasses neighbourhood planning, green corridors, transport systems, street orientation, and urban ventilation zones.

By proposing a replicable methodological framework for evaluating and enhancing OTC, this study intends to contribute to the advancement of urban climate resilience research and practice. Furthermore, it advocates for the strategic use of advanced simulation tools to guide the creation of sustainable, resilient, and age-inclusive urban environments that promote well-being and long-term liveability.

Author Contributions: Conceptualisation, M.I.A., R.K., H.C., F.G., P.C., S.C., L.B., C.R., F.A., A.S.N.R., R.J.G.R., G.L., A.M., A.S.F., J.B.d.S., T.F., L.M., L.A., I.M. and E.C.; methodology, M.I.A. and H.C.; software, M.I.A.; formal analysis, M.I.A. and R.K.; investigation, M.I.A. and R.K.; resources, F.A. and H.C.; data curation, M.I.A. and H.C.; visualisation, M.I.A.; writing—original draft preparation, M.I.A.; writing—review and editing, H.C., R.K., P.C., R.J.G.R., G.L., A.M., A.S.F., S.C., A.S.N.R., L.B., F.G., F.A., C.R., J.B.d.S., T.F., L.M., L.A., I.M. and E.C.; funding acquisition, F.A.; M.I.A. conducted the research and drafted the manuscript under the guidance and supervision of H.C. and F.A. who provided overall conceptual leadership, methodological oversight, and critical revision of the text. All authors have read and agreed to the published version of the manuscript.

Funding: This work was financially supported by national funds through the FCT/MCTES (PIDDAC), under the project PTDC/GES-URB/2038/2021—CAOP—CLIMATE ADAPTATION FOR OLDER PEOPLE LIVING IN VULNERABLE URBAN AREAS. Designing a climate-responsive and community-based methodology, with DOI (https://doi.org/10.54499/PTDC/GES-URB/2038/2021). This article was developed with the support of the Research Center for Territory, Transports and Environment (CITTA) of the Faculty of Engineering of the University of Porto, funded by Fundação para a Ciência e a Tecnologia, I.P./MECI through the national funds, UID/04427, of the CONSTRUCT—Institute of R&D in Structures and Construction—funded by Fundação para a Ciência e a Tecnologia, I.P./MECI, through the national funds, UID/04708/2025, of the Center for Studies Nuno Portas, funded by national funds through FCT—Fundação para a Ciência e a Tecnologia, I.P., under the project/grant UID/00145—CENP and of the RISE—Health, Competence Center for Active and Healthy Ageing, Faculty of Pharmacy, University of Porto.

Institutional Review Board Statement: Not applicable.

Informed Consent Statement: Not applicable.

Data Availability Statement: The original contributions presented in this study are included in the article. Further inquiries can be directed to the corresponding authors.

Acknowledgments: During the preparation of this work, the author(s) used Gemini 3 for the purposes of the interpretation of the spatial distribution maps and Quillbot v40 for the purposes of text editing (e.g., grammar, structure, spelling, punctuation and formatting). After using this tool/service, the author(s) reviewed and edited the content as needed and take(s) full responsibility for the content of the publication. The authors acknowledge the contribution of the reviewers and the editor.

Conflicts of Interest: The authors declare that they have no known competing financial interests or personal relationships that could have appeared to influence the work reported in this paper.

Abbreviations

The following abbreviations are used in this manuscript:

UHI	Urban Heat Island
OTC	Outdoor Thermal Comfort
CFD	Computational Fluid Dynamics
PET	Physiological Equivalent Temperature
OUT_SET	Outdoor Standard Effective Temperature
UTCI	Universal Thermal Climate Index
PMV	Predicted Mean Vote
Ta	Air Temperature
Ws	Wind Speed
RH	Relative Humidity
MRT	Mean Radiant Temperature
SVF	Sky View Factor
Ts	Surface Temperature
PS	Public Space
ES	Existing Scenario
TS	Tested Scenario

References

1. Eurostat. *Eurostat Regional Yearbook—2025 Edition*; Eurostat: Luxembourg, 2025.
2. United Nations. *World Urbanization Prospects: The 2025 Revision: Summary of Results*; UN DESA/POP/2025/TR/NO. 12; United Nations: New York, NY, USA, 2025.
3. Calvin, K.; Dasgupta, D.; Krinner, G.; Mukherji, A.; Thorne, P.W.; Trisos, C.; Romero, J.; Aldunce, P.; Barrett, K.; Blanco, G.; et al. *Climate Change 2023: Synthesis Report. Sixth Assessment Report of the Intergovernmental Panel on Climate Change*; Intergovernmental Panel on Climate Change: Geneva, Switzerland, 2023.

4. Arnfield, A.J. Two Decades of Urban Climate Research: A Review of Turbulence, Exchanges of Energy and Water, and the Urban Heat Island. *Int. J. Climatol.* **2003**, *23*, 1–26. [CrossRef]
5. Bowler, D.E.; Buyung-Ali, L.; Knight, T.M.; Pullin, A.S. Urban Greening to Cool Towns and Cities: A Systematic Review of the Empirical Evidence. *Landsc. Urban Plan.* **2010**, *97*, 147–155. [CrossRef]
6. Oke, T.R. The Energetic Basis of the Urban Heat Island. *Q. J. R. Meteorol. Soc.* **1982**, *108*, 1–24. [CrossRef]
7. Landsberg, H.E. *The Urban Climate*; Academic Press: New York, NY, USA; Toronto, ON, Canada, 1981.
8. Erell, E.; Pearlmutter, D.; Williamson, T. *Urban Microclimate—Designing the Spaces Between Buildings*; Routledge: London, UK, 2012; ISBN 9781136539435.
9. Gartland, L.M. *Heat Islands—Understanding and Mitigating Heat in Urban Areas*; Routledge: London, UK, 2012; ISBN 9781136564215.
10. Santamouris, M. On the Built Environment—The Urban Influence. In *Energy and Climate in the Urban Built Environment*; Santamouris, M., Ed.; Routledge: New York, NY, USA, 2001; pp. 3–18.
11. Papangelis, G.; Tombrou, M.; Dandou, A.; Kontos, T. An Urban "Green Planning" Approach Utilizing the Weather Research and Forecasting (WRF) Modeling System. A Case Study of Athens, Greece. *Landsc. Urban Plan.* **2012**, *105*, 174–183. [CrossRef]
12. Borrego, C.; Pio, C.; Rocha, A.; Miranda, A.; Castanheira, J.; Lopes, M.; Tchepel, O.; Martins, H.; Amorim, J.; Valente, J.; et al. *CLICURB—Qualidade da Atmosfera Urbana, Alterações Climáticas e Resiliência*; University of Aveiro: Aveiro, Portugal, 2015.
13. Srivastava, V.T.; Sharma, A.; Jadon, S.S. A Review of the Formation, Mitigation Strategies from 50 Years of Global Urban Heat Island Studies. *Environ. Dev. Sustain.* **2024**, *28*, 97–114. [CrossRef]
14. Li, S.; Zou, B.; Ma, X.; Liu, N.; Zhang, Z.; Xie, M.; Zhi, L. Improving Air Quality through Urban Form Optimization: A Review Study. *Build. Environ.* **2023**, *243*, 110685. [CrossRef]
15. Liu, B.; Guo, X.; Jiang, J. How Urban Morphology Relates to the Urban Heat Island Effect: A Multi-Indicator Study. *Sustainability* **2023**, *15*, 10787. [CrossRef]
16. Fallmann, J.; Emeis, S. How to Bring Urban and Global Climate Studies Together with Urban Planning and Architecture? *Dev. Built Environ.* **2020**, *4*, 100023. [CrossRef]
17. Figueiredo, T.; Midão, L.; Sampaio, R.; Carrilho, J.; Coelho, C.; Cerullo, G.; Di Paola, A.; Carfì, A.; Onder, G.; Costa, E. Managing Non-Cancer Chronic Pain in Frail Older Adults: A Pilot Study Based on a Multidisciplinary Approach. *Int. J. Environ. Res. Public Health* **2023**, *20*, 7150. [CrossRef]
18. Monteiro, A.; Sousa, C.; Fonseca, L.; Almeida, M.; Velho, S.; Carvalho, V. *Atlas Da Saúde e Da Doença: Vulnerabilidades Climáticas e Socioeconómicas Na Grande Área Metropolitana Do Porto e Concelho Do Porto*; CHERG: Porto, Portugal, 2012; Volume I–II, ISBN 978-989-98681-2-0.
19. Yang, X.; Zhao, L.; Bruse, M.; Meng, Q. An Integrated Simulation Method for Building Energy Performance Assessment in Urban Environments. *Energy Build.* **2012**, *54*, 243–251. [CrossRef]
20. Tsoka, S.; Tsikaloudaki, A.; Theodosiou, T. Analyzing the ENVI-Met Microclimate Model's Performance and Assessing Cool Materials and Urban Vegetation Applications—A Review. *Sustain. Cities Soc.* **2018**, *43*, 55–76. [CrossRef]
21. Lai, D.; Lian, Z.; Liu, W.; Guo, C.; Liu, W.; Liu, K.; Chen, Q. A Comprehensive Review of Thermal Comfort Studies in Urban Open Spaces. *Sci. Total Environ.* **2020**, *742*, 140092. [CrossRef]
22. Gonzalez, R.R.; Nishi, Y.; Gagge, A.P. Experimental Evaluation of Standard Effective Temperature a New Biometeorological Index of Man's Thermal Discomfort. *Int. J. Biometeorol.* **1974**, *18*, 1–15. [CrossRef]
23. Gagge, A.P.; Fobelets, A.P.; Berglund, L.G. A Standard Predictive Index of Human Response to the Thermal Environment. *ASHRAE Trans.* **1986**, *92*, 709–731.
24. Mayer, H.; Höppe, P. Thermal Comfort of Man in Different Urban Environments. *Theor. Appl. Climatol.* **1987**, *38*, 43–49. [CrossRef]
25. Höppe, P. The Physiological Equivalent Temperature—A Universal Index for the Biometeorological Assessment of the Thermal Environment. *Int. J. Biometeorol.* **1999**, *43*, 71–75. [CrossRef] [PubMed]
26. Jendritzky, G.; de Dear, R.; Havenith, G. UTCI—Why Another Thermal Index? *Int. J. Biometeorol.* **2012**, *56*, 421–428. [CrossRef] [PubMed]
27. Blazejczyk, K.; Epstein, Y.; Jendritzky, G.; Staiger, H.; Tinz, B. Comparison of UTCI to Selected Thermal Indices. *Int. J. Biometeorol.* **2012**, *56*, 515–535. [CrossRef]
28. Fanger, P.O. *Thermal Comfort: Analysis and Applications in Environmental Engineering*; McGraw-Hill: Columbus, OH, USA, 1970; ISSN 0070199159.
29. Deb, C.; Alur, R. Review of Studies on Outdoor Thermal Comfort Using Physiological Equivalent Temperature (PET). *J. Inst. Eng.* **2011**, *92*, 38–41.
30. Ali-Toudert, F.; Mayer, H. Effects of Asymmetry, Galleries, Overhanging Façades and Vegetation on Thermal Comfort in Urban Street Canyons. *Sol. Energy* **2007**, *81*, 742–754. [CrossRef]
31. Deb, C.; Alur, R. The Significance of Physiological Equivalent Temperature (PET) in Outdoor Thermal Comfort Studies. *Int. J. Eng. Sci. Technol.* **2010**, *2*, 2825–2828.

32. Matzarakis, A.; Rutz, F.; Mayer, H. Modelling Radiation Fluxes in Simple and Complex Environments—Application of the RayMan Model. *Int. J. Biometeorol.* **2007**, *51*, 323–334. [CrossRef] [PubMed]
33. Liu, W.; Zhang, Y.; Deng, Q. The Effects of Urban Microclimate on Outdoor Thermal Sensation and Neutral Temperature in Hot-Summer and Cold-Winter Climate. *Energy Build.* **2016**, *128*, 190–197. [CrossRef]
34. Tsitoura, M.; Tsoutsos, T.; Daras, T. Evaluation of Comfort Conditions in Urban Open Spaces. Application in the Island of Crete. *Energy Convers. Manag.* **2014**, *86*, 250–258. [CrossRef]
35. Lai, D.; Guo, D.; Hou, Y.; Lin, C.; Chen, Q. Studies of Outdoor Thermal Comfort in Northern China. *Build. Environ.* **2014**, *77*, 110–118. [CrossRef]
36. Cheng, V.; Ng, E.; Chan, C.; Givoni, B. Outdoor Thermal Comfort Study in a Sub-Tropical Climate: A Longitudinal Study Based in Hong Kong. *Int. J. Biometeorol.* **2012**, *56*, 43–56. [CrossRef]
37. Nikolopoulou, M.; Baker, N.; Steemers, K. Thermal Comfort in Outdoor Urban Spaces: Understanding the Human Parameter. *Sol. Energy* **2001**, *70*, 227–235. [CrossRef]
38. Middel, A.; Chhetri, N.; Quay, R. Urban Forestry and Cool Roofs: Assessment of Heat Mitigation Strategies in Phoenix Residential Neighborhoods. *Urban For. Urban Green.* **2015**, *14*, 178–186. [CrossRef]
39. ISO. *Ergonomics of the Thermal Environment-Instruments for Measuring Physical Quantities*; ISO: Geneva, Switzerland, 1998.
40. Kántor, N.; Unger, J. The Most Problematic Variable in the Course of Human-Biometeorological Comfort Assessment—The Mean Radiant Temperature. *Open Geosci.* **2011**, *3*, 90–100. [CrossRef]
41. Johansson, E.; Spangenberg, J.; Gouvêa, M.L.; Freitas, E.D. Scale-Integrated Atmospheric Simulations to Assess Thermal Comfort in Different Urban Tissues in the Warm Humid Summer of São Paulo, Brazil. *Urban Clim.* **2013**, *6*, 24–43. [CrossRef]
42. Lin, T.; de Dear, R.; Hwang, R. Effect of Thermal Adaptation on Seasonal Outdoor Thermal Comfort. *Int. J. Climatol.* **2011**, *31*, 302–312. [CrossRef]
43. Liu, Z.; Li, J.; Xi, T. A Review of Thermal Comfort Evaluation and Improvement in Urban Outdoor Spaces. *Buildings* **2023**, *13*, 3050. [CrossRef]
44. Santamouris, M.; Gaitani, N.; Spanou, A.; Saliari, M.; Giannopoulou, K.; Vasilakopoulou, K.; Kardomateas, T. Using Cool Paving Materials to Improve Microclimate of Urban Areas—Design Realization and Results of the Flisvos Project. *Build. Environ.* **2012**, *53*, 128–136. [CrossRef]
45. Santamouris, M.; Synnefa, A.; Karlessi, T. Using Advanced Cool Materials in the Urban Built Environment to Mitigate Heat Islands and Improve Thermal Comfort Conditions. *Sol. Energy* **2011**, *85*, 3085–3102. [CrossRef]
46. Santamouris, M. Using Cool Pavements as a Mitigation Strategy to Fight Urban Heat Island—A Review of the Actual Developments. *Renew. Sustain. Energy Rev.* **2013**, *26*, 224–240. [CrossRef]
47. Erell, E. The Application of Urban Climate Research in the Design of Cities. *Adv. Build. Energy Res.* **2008**, *2*, 95–121. [CrossRef]
48. Toparlar, Y.; Blocken, B.; Maiheu, B.; van Heijst, G.J.F. A Review on the CFD Analysis of Urban Microclimate. *Renew. Sustain. Energy Rev.* **2017**, *80*, 1613–1640. [CrossRef]
49. Lai, Y.; Ning, Q.; Ge, X.; Fan, S. Thermal Regulation of Coastal Urban Forest Based on ENVI-Met Model—A Case Study in Qinhuangdao, China. *Sustainability* **2022**, *14*, 7337. [CrossRef]
50. Blocken, B. 50 Years of Computational Wind Engineering: Past, Present and Future. *J. Wind Eng. Ind. Aerodyn.* **2014**, *129*, 69–102. [CrossRef]
51. Mirzaei, P.A.; Haghighat, F. Approaches to Study Urban Heat Island—Abilities and Limitations. *Build. Environ.* **2010**, *45*, 2192–2201. [CrossRef]
52. Ooka, R. Recent Development of Assessment Tools for Urban Climate and Heat-island Investigation Especially Based on Experiences in Japan. *Int. J. Climatol.* **2007**, *27*, 1919–1930. [CrossRef]
53. Sola, A.; Corchero, C.; Salom, J.; Sanmarti, M. Simulation Tools to Build Urban-Scale Energy Models: A Review. *Energies* **2018**, *11*, 3269. [CrossRef]
54. Ng, E.; Chen, L.; Wang, Y.; Yuan, C. A Study on the Cooling Effects of Greening in a High-Density City: An Experience from Hong Kong. *Build. Environ.* **2012**, *47*, 256–271. [CrossRef]
55. Pordata, Resident Population, Estimates at December 31st: Total and by Sex. Last Updated in December 2025. Available online: https://www.pordata.pt/en/municipalities/resident+population++estimates+at+december+31st+total+and+by+sex-136 (accessed on 6 March 2026).
56. Monteiro, A.; Madureira, H.; Fonseca, L.; Velho, S. *Suporte Biofísico e Ambiente. Clima e Ambiente Urbano. Relatório de Caracterização e Diagnóstico*; Câmara Municipal do Porto. Direção Municipal de Urbanismo: Porto, Portugal, 2018.
57. INE. Census 2021—XVI Population Census. VI Housing Census. Available online: https://www.ine.pt/xurl/pub/65586079 (accessed on 16 January 2026).
58. Silva, J.B.; Tini, B.; Martins, A.; Mimoso, I.; Figueiredo, T.; Fernandes, A.S.; Gaspar, F.; Lameira, G.; Midão, L.; Alcântara, L.; et al. Participatory Methods to Support Climate Adaptation for Older Adults Living in Vulnerable Urban Areas: An Ethnographic Study. *Int. J. Environ. Res. Public Health* **2025**, *22*, 850. [CrossRef] [PubMed]

59. Boussaidi, K.; Djaghrouri, D.; Benabbas, M.; Altan, H. Assessment of Outdoor Thermal Comfort in Urban Public Space, during the Hottest Period in Annaba City, Algeria. *Sustainability* **2023**, *15*, 11763. [CrossRef]
60. Wang, Y.; Berardi, U.; Akbari, H. Comparing the Effects of Urban Heat Island Mitigation Strategies for Toronto, Canada. *Energy Build.* **2016**, *114*, 2–19. [CrossRef]
61. Taleghani, M.; Berardi, U. The Effect of Pavement Characteristics on Pedestrians' Thermal Comfort in Toronto. *Urban Clim.* **2018**, *24*, 449–459. [CrossRef]
62. Müller, N.; Kuttler, W.; Barlag, A.-B. Counteracting Urban Climate Change: Adaptation Measures and Their Effect on Thermal Comfort. *Theor. Appl. Climatol.* **2014**, *115*, 243–257. [CrossRef]